LWT - Food Science and Technology 168 (2022) 113929

Contents lists available at ScienceDirect

LWT

journal homepage: www.elsevier.com/locate/lwt

Evaluation of *in vitro* digestion methods and starch structure components as determinants for predicting the glycemic index of rice

Putlih Adzra Pautong [a,b,c,1], Joanne Jerenice Añonuevo [a,1], Maria Krishna de Guzman [a], Rodolfo Sumayao Jr. [b], Christiani Jeyakumar Henry [d], Nese Sreenivasulu [a,*]

[a] International Rice Research Institute, Los Baños, 4030, Philippines
[b] De La Salle University, Department of Chemistry, Manila, 0922, Philippines
[c] Mindanao State University, Gen. Santos City, 9500, Philippines
[d] Clinical Nutrition Research Centre, Singapore Institute for Clinical Sciences, 14 Medical Drive, #07-02, Singapore

ARTICLE INFO

Keywords:
Rice
Glycemic index
In vitro digestion
Starch fractions
Debranched starch

ABSTRACT

Mainstreaming the low glycemic index (GI) trait in breeding programs is constrained by low-throughput and high-cost clinical GI phenotyping. This study aimed to evaluate the potential of starch fine structure components and simulated digestion parameters in predicting GI in rice. Amylose (AM1 and AM2; $r = -0.94$ and $r = -0.80$, respectively, $p < .05$) and amylopectin fine structure (MCAP, SCAP, and SCAP1; $r = 0.78$-0.86, $p < .05$) measured through size-exclusion chromatography along with resistant starch ($r = -0.81$, $p < .05$) in seven (7) rice accessions showed high correlation with *in vivo* GI. Meanwhile, starch hydrolysis extent (SH) and the corresponding area under the digestion curve (AUC) obtained through *in vitro* digestion were found to be of higher correlation with GI, even within shorter digestion periods of 5 min or 30 min ($r = 0.96$, $p < .01$). These results highlight the potential use of these parameters as predictors of GI, with improved predictive capacity through a multiple regression model. Higher correlations of simulated digestion AUC with GI may be due to its ability to account for the overall food matrix native macro- and micro-structures, gaining an added advantage over SEC method as a predictive tool in studying rice GI variability. Validation in a larger population is an inevitable next step.

1. Introduction

Shift in dietary practices and lower energy expenditure brought about by various socio-economic developments linked with urbanization has led to the emergence of obesity as a serious global concern. Recent statistics reported that 1.9 billion adults are overweight; of them 422 million have diabetes (World Health Organization, 2020). Consuming energy-rich foods and drinks create chronic hyperglycemia (Yan, 2014). Obesity and hyperglycemia contribute to the increased incidences of non-communicable diseases (NCDs) like diabetes, cardiovascular diseases (CVDs), hypertension, and some cancers, among others, which account for more than 70% of annual deaths worldwide (World Health Organization, 2021).

Starch is the major source of carbohydrate in the diet. Interestingly, not all starches are created equal due to various intrinsic and extrinsic factors affecting their digestibility (Jukanti, Pautong, Liu, & Sreenivasulu, 2020; Toutounji, Farahnaky, et al., 2019). Slow starch digestibility is an important target trait in food since high postprandial glucose levels have been associated with various non-communicable diseases such as obesity, type 2 diabetes, and cardiovascular diseases (Blaak et al., 2012). Monitoring the quality of carbohydrates (which account for 40–80% of daily energy intake) is an essential intervention for glycemic control. More than half of the global population, mainly in Asia, derives more than 50% of daily calories from rice (GRiSP, 2013). Incidentally, 60% of people with diabetes live in the continent (Nanditha et al., 2016), making rice a vital food component in diet-based solutions to the growing epidemic of diabetes, at least for rice-consuming populations.

Starch-rich cereals which include rice are typically of intermediate to high GI (Anacleto et al., 2019; Fitzgerald et al., 2011; Kaur, Ranawana, & Henry, 2016; Miller, Pang, & Bramall, 1992). In rice-based diets, reducing the glycemic index (GI) of a variety through genetics, post-harvest processing, cooking, and diet diversification solutions are critical (Jukanti et al., 2020). GI is a clinical measure of the tendency of food or drinks containing 50 g of available carbohydrates to influence the

* Corresponding author.
E-mail address: n.sreenivasulu@irri.org (N. Sreenivasulu).
[1] These authors contributed to this work equally as co-first authors.

https://doi.org/10.1016/j.lwt.2022.113929
Received 13 April 2022; Received in revised form 24 August 2022; Accepted 3 September 2022
Available online 8 September 2022

blood glucose response upon intake relative to the same amount of glucose standard (Jenkins et al., 1981). GI classifies food as low (≤55), intermediate (>55–69), or high GI (≥70) (Atkinson, Foster-Powell, & Brand-Miller, 2008).

With more than half of the global population being dependent on rice as a staple carbohydrate source, it is crucial that low GI rice cultivars are made available to consumers to ease the burden of NCDs. To breed low GI varieties, (a) understanding of the genetics of glycemic index in rice through genome-phenotype associations and identifying diagnostic markers and (b) a rapid high-throughput GI phenotyping exhibiting higher correlations with gold standard *in vivo* clinical method are prerequisites. The lack of a low-cost, high-throughput *in vitro* method to replace the gold standard *in vivo* GI screening with human volunteers, which is both expensive and time-consuming, remains a serious limitation. To date, *in vitro* technique to estimate GI has been described by Goñi, Garcia-Alonso, and Saura-Calixto (1997), which makes use of gastrointestinal enzymes pepsin, pancreatic α-amylase (AA), and amyloglucosidase (AMG) in the digestion of common dietary starchy foods. Briefly, glucose released through hydrolysis is quantified as a percentage of starch hydrolyzed at different time points (SH) typically 0–180 min at 30 min intervals. Taken from a plot of these values is the area under the digestion curve (AUC) of the test food, whose ratio (expressed in percentage) with the AUC of a reference food, is referred to as hydrolysis index (HI). Two equations from the experiments of Goñi et al. (1997) were found to best estimate *in vivo* GI values of the test foods used in their study: $GI = 39.21 + 0.803(SH_{90})$ (Equation 1, $r = 0.909$, $p \leq .05$) which can be used to estimate GI using hydrolysis value at a single time point (t = 90 min), and GI = 39.71 + 0549(Hl) of food but lower linear correlation (Equation 2, $r = 0.894$, $p \leq .05$) which makes use of HI derived from multiple time points less accurate. The said equations have been used in numerous studies to estimate the GI of various food matrices (Chung, Shin, & Lim, 2008; Germaine et al., 2008; Kim & White, 2012; Lal et al., 2021; Leoro, Clerici, Chang, & Steel, 2010) including rice (Deepa, Singh, & Naidu, 2010; Fernandes, Madalena, Pinheiro, & Vicente, 2020; Kale, Jha, Jha, Sinha, & Lal, 2015; Kunyanee & Luangsakul, 2018; Tutusaus, Srikaeo, & Diéguez, 2013). Although widely used, it should be noted that *in vitro* GI equations are derived from a wide range of food types with varying starch hydrolysis characteristics (Goñi et al., 1997) for which the hydrolytic process was found to follow the first-order equation $C{=}C_{\infty}(1\text{-}e^{-kt})$. However, some slowly digestible foodstuffs reach a plateau by 90 min of hydrolysis (essentially zero-order) and thus cannot be subjected to first-order kinetics analysis; which will otherwise result to unreliable C_{∞} values (Edwards, Cochetel, Setterfield, Perez-Moral, & Warren, 2019). Starch digestion is known to be affected primarily by starch multi-scale structure spanning hierarchical structural levels such as compositional, short-range, helical, crystalline, lamellar, and morphology structures, which is perhaps made further complex by proteins, lipids, and secondary metabolites that modify the said structures, as thoroughly reviewed elsewhere (Chi et al., 2021).

Several alternative protocols that differ in digestion conditions such as activities and incubation times were proposed (Brodkorb et al., 2019; Edwards et al., 2019; Fitzgerald et al., 2011; Germaine et al., 2008; Toutounji, Butardo, et al., 2019). In contrast to methods that aim to compare GI across various food matrices such as the INFOGEST method (Brodkorb et al., 2019), a protocol intended for a specific food such as rice could benefit from lower variability in food matrix composition and structure due to a more narrow range of protein (4.91%–12.08%) (Banerjee, Chandel, Mandal, Meena, & Saluja, 2011) and lipids (0.5%–0.8%) (Juliano, 1985, pp. 59–174) compared to a wider range when comparison is made across various botanic sources.

Moreover, the association between GI and starch digestion rate has been previously studied by Englyst, Vinoy, Englyst, and Lang (2003). They classified starch into fractions that differ in their rate of hydrolysis in the small intestine: rapidly digestible starch (RDS), slowly digestible starch (SDS), and resistant starch (RS) that are hydrolyzed within the first 20 min, between 20 and 120 min, and remains undigested after 120 min, respectively. Furthermore, correlations between these fractions and amylopectin fine structure have been examined in rice (Benmoussa, Moldenhauer, & Hamaker, 2007), where among the amylopectin fractions, those with degrees of polymerization (DP) of less than 13 showed a positive correlation with RDS while longer DPs showed negative correlation.

Based on these premises, we hypothesize that fine structure components of amylose (AM1 and AM2) and amylopectin (medium-chain MCAP, short-chain SCAP, and its subfractions SCAP1, SCAP 2, and SCAP 3, that differ in degrees of polymerization) can be used to predict the GI in rice. We further hypothesize that *in vitro* amylolysis protocols employing low sample requirements, shorter digestion period, and/or lower enzyme activities can be modified for rice samples such that amylolysis parameters SH and AUC strongly correlate with *in vivo* GI. The purpose of the study was to evaluate and compare the performance of these methods for predicting the GI in rice. A reliable, high-throughput, and more affordable GI phenotyping method may fast-track the research efforts on understanding the genetics of GI in rice, with the ultimate goal of mainstreaming this human health-promoting trait in rice breeding programs.

2. Materials and methods

2.1. Samples

The milled rice samples of seven *indica* rice cultivars previously validated through *in vivo* GI estimation through human subjects (Anacleto et al., 2019; Pasion et al., 2021) were used to establish *in vitro* GI prediction methods. These cultivars include GQ02522 (50.4, low), GQ02497 (51.5, low), IRRI147 (55, low), IRRI162 (57, intermediate), IRRI163 (64, intermediate), IR64 (66, intermediate) and IR65 (90, high).

Meanwhile, the variability of predicted GI values across various linear regression models and parameters was then demonstrated using 10 market samples, of these three are brown rice and the rest are milled (Table 5).

2.2. Profiling of starch indices and debranched starch regions

Starch indices such as total starch (TS), digestible carbohydrates (DC) and resistant starch (RS) were measured using commercially available kits (Megazyme K-TSTA and K-RSTAR) with downscaled enzyme buffers as described in Alhambra, Dhital, Sreenivasulu, and Butardo (2019) with minor modification. Meanwhile, the starch regions (AM1, AM2, MCAP, and SCAP) were characterized using size exclusion chromatography following the procedures described in Guzman et al. (2017).

2.2.1. Total starch (TS) quantification

Rice flour (10 ± 0.1 mg) weighed in 2-mL microfuge tubes was dispersed in 0.5 mL of 80% (w/v) ethanol and incubated at 85 °C for 5 min. Another 0.5 mL of 80% ethanol was added followed by centrifugation at 3000 rpm for 10 min. After carefully decanting the supernatant, the pellet was re-suspended with 1 mL of 80% ethanol. After another centrifugation step, the supernatant was decanted once again, and the remaining pellet was added with 0.2 mL of 2M KOH. A magnetic spin bar was added to aid mixing, and solubilization of the pellet was allowed to proceed for at least 20 min in an ice bath. After the incubation, 0.8 mL of 1.2 M sodium acetate buffer (pH 3.8) was added followed by the addition of 10 μL each of thermostable α-amylase and AMG. The sample was then incubated at 50 °C for 30 min with intermittent vortex mixing every 15 min. After the enzymatic hydrolysis, an aliquot (0.1 mL) was added with distilled water to bring the final volume to 1 mL. The mixture was mixed and centrifuged at 13,000 rpm for 10 min. An aliquot (10 μL) of the supernatant was mixed with 0.3 mL of GOPOD reagent,

incubated at 50 °C for 20 min, and absorbance was read at 510 nm using a microplate reader (SPECTROstar Nano, BMG Labtech, Germany).

2.2.2. Resistant starch (RS) quantification

Rice flour samples (10 ± 0.1 mg) weighed in a 2-mL microfuge tubes were dispersed in 0.4 mL of enzyme solution containing 10 mg/mL pancreatin and 3 U/mL AMG in 0.1 mM sodium maleate buffer with 5 mM $CaCl_2 \cdot H_2O$ (pH 6.0). The tubes were then secured on a rack and incubated horizontally in a shaking water bath set at 100 strokes/min and 37 °C for 16 h. Twelve minutes prior to the end of the incubation period, the tubes were removed from the water bath and individually dried using a paper towel. At exactly 16 h, the reaction was stopped by adding 0.4 mL of 99% ethanol followed by vortex mixing. The tubes were centrifuged at 18,231×*g* for 30 min. The supernatant was then carefully decanted in a 15-mL conical tube and was set aside for the quantification of total digestible carbohydrate (DC). The remaining pellet was then re-suspended in 0.2 mL of 50% ethanol and mixed using a vortexer and added with a further 0.6 mL of 50% ethanol. Following another centrifugation, the supernatant was carefully decanted into the conical tube containing the first decantate, pooling both decantates together. On the other hand, a stir bar was placed in the tube containing the pellet over an ice bath and 0.2 mL of 2 M KOH was added, allowing complete solubilization for at least 20 min. At the end of the reaction time, 0.8 mL of 1.2 M sodium acetate buffer (pH 3.8) was added followed by the immediate addition of 10 μL of AMG (3300 U/mL). After mixing, the tubes were incubated in a water bath at 50 °C for 30 min (with vortex mixing after the first 15 min). Without the stir bars, the tubes were then centrifuged at 18,231×*g* for 10 min, and glucose concentration in a 10-μL aliquot of the resulting supernatant was quantified as in the preceding section.

2.2.3. Total digestible carbohydrates (DC)

The pooled supernatants (previous section) were diluted to 10 mL with 0.1 mM sodium acetate buffer (pH 4.5). After mixing, a 10-μL aliquot was collected, added with 2 μL of AMG suspension (300 U/mL in 100 mM sodium maleate buffer with 5 mM $CaCl_2 \cdot 2H_2O$; pH 6.0) and the mixture was vortexed and incubated in a 50 °C water bath for 20 min. Glucose was then quantified using GOPOD reagent (0.3 mL) as in 2.2.1.

2.2.4. Profiling of debranched starch

Waters Alliance 2695 HPLC with 2414 Refractive Index Detector and fitted with Waters Ultrahydrogel 250 Å column was first calibrated for molecular weight using pullulan standards (P-82 Shodex, Showa Denko, K. K. Kawasaki, Japan). Mark-Houwink-Sakurada equation for universal calibration (Pullulan: $K = 0.0126$ mL g^{-1} and a = 0.733; Linear starch: $K = 0.0544$ mL g^{-1} and a = 0.486) as described in Castro, Dumas, Chiou, Fitzgerald, and Gilbert (2005) was used with 0.05M NH_4OAc with 0.02% sodium azide (pH 4.75) as mobile phase.

Gelatinization of rice flour (50 ± 0.1 mg in a glass scintillation vial of known weight) was done by adding 0.4 mL of 95% ethanol and 1 mL of 0.25 M NaOH, followed by heating at 150 °C for 12 min. Within the heating period, successive aliquots of 0.8 mL hot water (100 °C) were added at 0, 4, and 8 min from the onset of heating period to prevent drying of sample. After heating, the final weight of the solution was adjusted to 4 g by adding hot water (60–65 °C). Debranching of the gelatinized starch was then induced by adding 0.206 mL of sodium acetate buffer (prepared by mixing 10 mL 0.2M NaOAc at pH 4.0 with 0.360 mL glacial acetic acid) to a 0.794-mL aliquot of the sample. The resulting mixture was then incubated with 10 μL of isoamylase (P113541, Megazyme) in a 50 °C water bath for 2 h with mixing by inversion every 15 min. Isoamylase was then inactivated by placing the tubes in a vigorously boiling water bath. After centrifugation at 12,5000×*g* for 10 min, the supernatant is carefully decanted into a 1.5-mL microfuge tube containing ~0.1 g ion exchange resin (Bio-Rad AG 501-X8 (D)) which was then incubated at 50 °C for 30 min (with mixing by inversion every 10 min). An aliquot (0.15 mL) of the supernatant was then transferred to an SEC vial for analysis (stop time, 35 min; flow rate, 0.5 mL/min; injection volume, 40 μL; sample temperature, 40 °C; and column temperature, 60 °C). The degree of polymerization (DP) was derived from the molecular weight computed using the Mark-Houwink-Sakurada Equation, and the four regions were determined using this distribution: AM1>1000DP, AM2 121-1000DP, MCAP 37-120DP, and SCAP 6-36DP. SCAP was further distributed into three regions, SCAP1 25-36DP, SCAP2 13-24DP, and SCAP3 6-12DP, based on Hanashiro, Abe, and Hizukuri (1996).

2.3. In vitro starch digestion protocols

Three different *in vitro* GI methods were standardized for sample preparation, digestion, and/or glucose quantification in this study (Table 2).

2.3.1. Method 1

A slightly modified version of the procedure by Goñi et al. (1997) was employed to test its applicability in rice using reference samples of seven cultivars with established *in vivo* GI (Anacleto et al., 2019; Pasion et al., 2021). In addition, Method 1 was modified (referred to as Modified Method 1) by incorporating the following changes: whole grains (100 ± 5 mg) were used instead of flour (50 mg, passed through a 425 μm mesh), a 1:2 rice to water ratio was used instead of 3 mL water, and all incubations were conducted at 37 °C to simplify the process, as opposed to the two incubation temperatures in the original Method 1.

Briefly, rice grains (100 ± 0.3 mg) were added with 0.2 ml distilled water and cooked for 23 min over vigorously boiling water in a covered pot. The cooked sample was then allowed to cool down for 5 min and equilibrated in a 37 °C water bath for another 5 min. The grains were then minced in 0.5 ml of HCl–KCl buffer (0.05 M, pH 1.5) using a stainless steel spatula with 20 downward strokes. Then, 9.7 ml of HCl–KCl buffer (0.05 M, pH 1.5) containing 40 U of pepsin (Sigma; 4.12 U/mL or 95.9 μg/mL) was added and allowed to incubate for 1 h with constant magnetic stirring (90 rpm). The pH was then adjusted to 6.9 by adding 2 mL of aqueous NaOH (~0.163 M), followed by the addition of 14.8 mL of Tris-maleate buffer (0,05 M, pH 6.9) containing 2.6 U of α-amylase (A3176, Sigma; 0.176 U/mL or 11.7 μg/mL). Starch hydrolysis was allowed to proceed for 180 min in the water bath (37 °C, 90 rpm). Sample aliquots (0.1 mL) were collected at 0, 30, 60, 90, 120, and 180 min and immediately placed in boiling water for 5 min to deactivate the enzymes. The aliquot was then centrifuged at 13,500 rpm for 10 min, and 10 μL of the resulting supernatant was added with 30 μL AMG (2.75 U/mL) in sodium acetate buffer (0.4 M, pH 4.75), vortexed, and incubated at 50 °C for 20 min to convert starch oligosaccharides into free glucose. After incubation, 60 μL of Milli-Q water was added, vortexed, and a 10-μL sub-aliquot was transferred into a 0.6-mL microfuge tube. Glucose was then quantified using a GOPOD reagent as in Section 2.2.1. A reagent blank was incubated under the same conditions, and absorbance at different time points was also measured to correct for interferences due to the digestion medium. The calculation of SH from glucose concentrations and predicted GI (pGI) value is described in Section 2.3.4.

2.3.2. Method 2

The second method employed the protocol reported by Alhambra et al. (2019) with modifications. Whole milled rice grains (500 ± 10 mg) were soaked for 10 min, and brown rice samples were soaked for 20 min in 6 mL distilled water using 50-mL tube with a foil cap, under room temperature. Afterwards, the sample was cooked in a beaker with boiling water (heater set at 250 °C) for 20 min. Excess water was removed, and rice was allowed to cool for 5 min. The tubes were then placed in a 37 °C water bath and 0.5 mL α-amylase (Megazyme; 75 U/mL in simulated salivary fluid) was dispensed. The grains were minced using a spatula for 20 s to mimic the buccal phase, followed by the addition of 5 mL pepsin (P6778, Sigma; 1 mg/mL in 0.2M HCl). Spin

bars were added, and the speed was set to 200 rpm. After 30 min, 5 mL of NaOH (0.2 M) was added to neutralize the pH, followed by the addition of 20 mL sodium acetate buffer (0.1 M, pH 6.0), and 5 mL pancreatin (P1750, Sigma; 2 mg/mL buffer)-AMG (10115-5G-F, Sigma; 25.4 U/mL or 0.41 mg/mL buffer) mixture while the speed of stirring was increased to 700 rpm. This reaction was allowed to carry out for 180 min, and 0.2 ml of aliquots were collected at time points 0, 5, 10, 20, 30, 45, 60, 90, 120, and 180 min, and placed in a 0.6 ml microfuge tube. To quench the reaction, the tubes were placed on an ice bath prior to centrifugation at 13,000 rpm (4 °C) for 10 min.

Samples were diluted with 0.1M sodium acetate buffer (pH 6.0) when needed (dilution starts at aliquots 5 min and beyond). Aliquots of 50 μl were added with 5 μL of amyloglucosidase (300 U/mL) and incubated for 20 min at 50 °C. Starch hydrolyzed was quantified using the GOPOD assay at 510 nm (Beckman Coulter DU 800 spectrophotometer). The calculation of predicted GI (pGI) value is described in Section 2.3.4.

2.3.3. Method 3

A third starch digestion protocol was employed following the method of Germaine et al. (2008) with some modifications. Briefly, whole milled rice (300 ± 0.3 mg) with 1:2 rice-to-water ratio was cooked in 50-ml tube over boiling water for 23 min, after which the sample was set aside at room temperature for 5 min. After equilibrating in a 37 °C water bath for another 5 min, it is added with 1 mL of 0.1 M sodium potassium phosphate buffer (pH 6.9) and minced using a stainless-steel spatula (35 downward strokes within 10 s). After placing a magnetic spin bar, 2 mL of α-amylase (A3176, Sigma; 55.5 U/mL or 3.7 mg/mL of 0.05 M sodium potassium phosphate buffer, pH 6.9, 37 °C) was added, and amylolysis was allowed for 75 s in a water bath with constant stirring (37°, 60 rpm). The reaction was stopped by adding 3 mL of aqueous HCl (pH ~0.92) to acidify the digestion medium. Then, 3 mL of pepsin (Sigma; 19.5 U/mL or 0.45 mg/mL of 0.1 M sodium potassium phosphate buffer, pH 1.5, 37 °C) was added and allowed to incubate for 30 min (37 °C water bath, 60 rpm). Enzymatic reaction was quenched by adjusting the pH to 6.9 using 15 mL of aqueous NaOH (pH ~12.6). A 15 mL enzyme solution containing pancreatin (28.4 μg/mL; P1750, Sigma) and amyloglucosidase (10115-5G-F, Sigma; 13 U/mL or 0.208 mg/mL) in 0.1 M sodium potassium phosphate buffer (pH 6.9) was then added and allowed to incubate for another 180 min (37 °C, 120 rpm). Sample aliquots (0.70 mL) were withdrawn at 0 (just before pancreatin-AMG addition), 30, 60, 90, 120, 150, and 180 min and placed on ice until the succeeding centrifugation step (13,500 rpm, 10 min, 4 °C). A 1-μL aliquot of the supernatant was transferred to a 0.6-mL microfuge tube and was added with 9 μL of AMG solution (33.3 U/mL in 0.4 M sodium acetate buffer, pH 5.0), vortexed, and incubated in a water bath (50 °C) for 20 min. Finally, glucose in the mixture and reagent blank were measured by adding GOPOD reagent and analyzed as in Method 1.

2.3.4. Calculation of starch hydrolyzed (SH), AUC, and derivation of pGI equations

Sample and glucose standard absorbance values at 510 nm were corrected using a reagent blank, and converted into glucose values (mg/ml of aliquot) using the following equation:

$$Glucose = Absorbance\ of\ sample / Absorbance\ of\ glucose\ standard\ x\ 100\ x\ 10/1000$$

where the fraction 10/1000 was used to convert mcg glucose/0.1 ml aliquot to mg/ml. The percentage of starch hydrolyzed (SH) was then calculated using the equation:

$$SH = (glucose\ x\ DF\ x\ V\ x\ 162\ /\ 180)/(sample\ weight\ x\ (\%TS)\ /\ 100)\ x\ 100$$

where glucose is in mg/ml, DF is the dilution factor used on the sample aliquot, V is the volume of the digestion medium at the time point during which the aliquot was drawn, 162/180 is the conversion factor from glucose to starch, and %TS is the total starch content of the sample. Finally, AUC was calculated from SH values based on the trapezoidal rule.

2.4. Derivation of linear regression predictive GI (pGI) equations

The Pearson correlation coefficient (r, $P < .05$; R package "corrplot" (Wei & Simko, 2021)) was used to assess the correlation between *in vivo* GI and each of the parameters tested. Following the tests for linearity (ANOVA for linear regression), normal distribution of the residuals of regression (Shapiro-Wilk; R package "dplyr"; Wickham, François, Henry, & Müller, 2022), and homoscedasticity (R package "lmtest"; Zeileis & Hothorn, 2002) of each parameter showing a good correlation with *in vivo* GI, linear regression analysis was then performed to generate the corresponding pGI equations and values. Statistical analysis was performed using RStudio 2022.2.3.492 (RStudio Team, 2020).

2.5. Evaluation of derived pGI equations on market samples

The applicability of the derived equations for predicted GI (pGI) using different amylolysis parameters were demonstrated for ten (10) market samples. SEC experiments were performed in triplicates while simulated digestion were performed in duplicates.

3. Results and discussion

3.1. Evaluation of starch indices and starch regions as proxy parameters to estimate GI

The range of starch indices (TS, RS, and DC) and debranched starch regions separated through SEC (AM1, AM2, MCAP, and SCAP and its subfractions) in seven (7) rice accessions are presented in Table 1. RS, AM1, and AM2 declined whereas MCAP, SCAP, and SCAP increased with increasing GI. On the contrary, no such statistically significant trends were observed for TS and DC ($p > .05$, Table S1). Although direct positive correlations (MCAP, $r = .780$; SCAP, $r = .855$; SCAP1, $r = 0.856$; AP, $r = .886$) and inverse correlations (RS, $r = -0.809$; AM1, $r = -0.941$; and AM2, $r = -0.802$) were observed with *in vivo* GI values (Fig. 1), they were found to be less than those achieved using amylolysis parameters SH and AUC for *in vitro* GI methods 2 and 3 (Fig. 4) even when individual fractions are pooled together (AM and AP, $r = -0.886$; AM_{AUC} and $AM_{AUC,}$ $r = -0.880$). This observation is also reflected in the corresponding R^2 values when linear regression model is applied (Fig. S1). Further inspection of the SCAP fractions revealed that GI was significantly correlated with SCAP1 only ($r = 0.856$, $p = .014$) which is slightly higher than that for the totality of SCAP ($r = 0.855$, $p = .014$). These parameters passed the assumptions of linearity with GI, and normal distribution and homoscedasticity of the corresponding residuals based on ANOVA, Shapiro-Wilk test and Breusch-Pagan test, respectively, which served as the bases for linear regression analysis (Table 3).

Based on these results, only RS, AM1, AM2, SCAP1, AM, and AM_{AUC} were used as proxy parameters in succeeding analyses (Section 3.3). AP

Table 1
Distribution of various starch parameters across seven (7) rice varieties.

Parameters	Samples						
	GQ02522 (GI = 50.4)	GQ02497 (GI = 51.5)	IRRI147 (GI = 55)	IRRI162 (GI = 57)	IRRI163 (GI = 64)	IR64 (GI = 66)	IR65 (GI = 90)
TS	85.21 ± 1.03	87.15 ± 0.68	85.94 ± 0.61	85.75 ± 1.17	83.34 ± 1.03	84.39 ± 1.23	85.79 ± 1.57
DC	83.14 ± 1.10	86.24 ± 1.87	83.66 ± 2.32	83.04 ± 4.30	85.79 ± 2.00	82.70 ± 2.64	86.27 ± 1.71
RS	2.08 ± 0.27	1.16 ± 0.14	1.66 ± 0.92	1.77 ± 0.46	1.01 ± 0.25	1.65 ± 0.38	0.29 ± 0.05
AM1	11.47 ± 2.10	11.31 ± 1.42	8.63 ± 1.47	7.45 ± 2.36	6.18 ± 1.37	6.18 ± 2.34	2.16 ± 1.30
AM2	14.24 ± 1.92	12.36 ± 2.35	11.02 ± 0.02	8.25 ± 0.72	6.64 ± 2.06	7.74 ± 1.16	5.71 ± 1.25
MCAP	24.81 ± 0.76	25.74 ± 0.55	26.38 ± 0.40	28.38 ± 1.86	28.69 ± 1.19	25.77 ± 0.71	30.34 ± 0.67
SCAP	49.48 ± 0.68	50.59 ± 4.32	53.97 ± 1.10	55.92 ± 1.81	58.49 ± 1.57	60.31 ± 1.34	61.79 ± 1.86
SCAP1	13.41 ± 0.40	13.95 ± 0.64	15.08 ± 0.01	15.35 ± 0.12	15.99 ± 1.26	15.46 ± 0.28	16.80 ± 0.35
SCAP2	28.96 ± 0.23	29.43 ± 2.67	32.86 ± 1.08	32.34 ± 1.17	33.62 ± 1.13	37.53 ± 1.09	36.09 ± 1.12
SCAP3	7.12 ± 0.28	7.21 ± 1.01	6.03 ± 0.00	8.22 ± 0.80	8.87 ± 0.82	7.33 ± 0.58	8.91 ± 0.73
AM	25.71 ± 0.58	23.67 ± 3.77	19.66 ± 1.50	15.70 ± 1.96	12.82 ± 2.76	13.92 ± 1.63	7.87 ± 1.81
AP	74.29 ± 0.58	76.33 ± 3.77	80.34 ± 1.50	84.30 ± 1.96	87.18 ± 2.76	86.08 ± 1.63	92.13 ± 1.81
AM_{AUC}	24.25 ± 0.88	20.91 ± 3.11	18.08 ± 1.83	14.00 ± 2.28	10.05 ± 0.52	12.90 ± 1.59	5.90 ± 1.83
AP_{AUC}	75.75 ± 0.88	79.09 ± 3.11	81.92 ± 1.83	86.00 ± 2.28	89.95 ± 0.52	87.10 ± 1.59	94.10 ± 1.83
AUC[a]	47.1 ± 6.1	38.4 ± 0.6	45.9 ± 5.8	63.5 ± 0.5	55.4 ± 1.4	83.2 ± 7.1	125.0 ± 30.5
AUC[b]	534 ± 86	551 ± 37	481 ± 57	615 ± 45	709 ± 140	866 ± 72	1703 ± 83

The values are expressed as the mean of six (6) replicates for TS and DC, five (5) for RS, and three (3) for SEC-derived parameters ± standard deviation. [a]AUC(0–5) from Method 2; [b]AUC(150–180) from Method 3; TS = Total Starch; DC = Digestible Carbohydrates; RS = Resistant Starch; AM1 = percent amylose (DP > 1000 to 20,000); AM2 = percent long-chain amylopectin (DP > 120 to 1000); MCAP = medium-chain amylopectin (DP > 36 to 120); SCAP = short-chain amylopectin (DP 6–36); SCAP1 (DP 6–12); SCAP2 (DP 13–24); SCAP3 (DP 25–36); AM (AM1+AM2); AP (MCAP + SCAP); AM_{AUC} and AP_{AUC} are percent amylose and amylopectin based on visual inspection of SEC peaks.

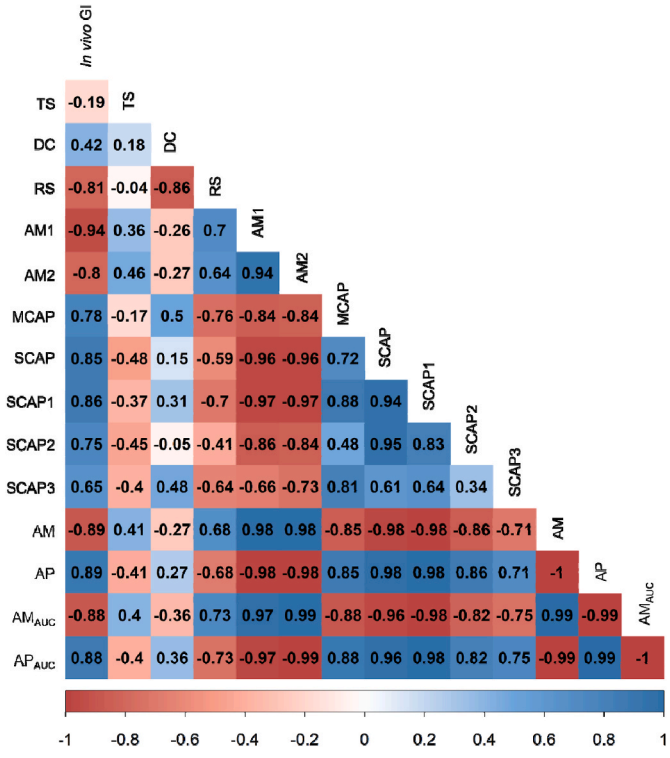

Fig. 1. Correlations between and among starch parameters and *in vivo* GI.

and AP_{AUC} were not included since they both give pGI equations with the same value of slope (but of opposite sign) as that of the pGI for AM and AM_{AUC} (Figs. S1h and S1j, respectively).

The trends in AM1 and AM2 (and collectively as AM or AM_{AUC}) in this study corroborate previously reported negative correlation between amylose and GI (Fitzgerald et al., 2011; Goñi et al., 1997; Guzman et al., 2017; Hu, Zhao, Duan, Linlin, & Wu, 2004) since low amylose digestibility is attributed to its linear nature that limits the surface area for hydrolytic enzyme action. In addition, amylose is known to provide the structural integrity to retard swelling and disruption of starch structure during cooking and reassemble into ordered structures upon cooling (Chi et al., 2021). While the DP of amylopectin has been shown to affect the digestibility of starch (Martens, Gerrits, Bruininx, & Schols, 2018; Srichuwong, Sunarti, Mishima, Isono, & Hisamatsu, 2005), we report a contrasting result with respect to MCAP which displayed a positive correlation with GI. This can be explained by the "*building block and backbone*" model of amylopectin structure (Bertoft, 2004; Perez & Bertoft, 2010) which suggests that DP > 36 (which includes MCAP) mostly interlink through α-(1,6)-linkages to form the backbone to which the building blocks of double helices of DP ≤ 36 (SCAP) are subtended. A huge proportion of the backbones are situated perpendicular to the crystalline clusters and are therefore mostly found in the amorphous lamella which is more accessible to hydrolytic enzymes.

In addition, among the SCAP sub-fractions, our results show that only SCAP1 (DP 25–36) is significantly positively correlated with GI, contrary to previously reported negative correlation with starch digestibility while positive correlations were observed for shorter SCAP fractions (DP 6–24) only (Lin et al., 2016; Srichuwong et al., 2005). This may imply that double helices formed by longer chains (DP 25–36) believed to have higher resistance (Nakamura, 2018) could exist as amorphous double helices (Kim, Choi, Choi, Park, & Moon, 2020) and may actually potentially cause uneven packing and thus reduce crystallinity, as more often attributed to shorter helices (Chi et al., 2021). DP 25–36 has been previously reported to introduce defects into the structure of rice starches (Koroteeva et al., 2007), and thus potentially increase digestibility which is consistent with our result. Moreover, the backbone model suggests that SCAP3 of DP 6–8 anchored to the backbone rather than the helical clusters or building blocks may be present, which may introduce defects in the crystalline structure. It is thus tempting to speculate that SCAP1 (DP 25–36) also contributes to such structural defects and to a greater extent. With these premises, superior haplotypes for *bHLH* transcription factor on chromosome 7 identified to elevate AM1 fraction over SCAP (Butardo et al., 2017) will be useful as a quick screening technique to enrich the germplasm of low GI potential from the gene bank accessions (Brotman et al., 2021).

Furthermore, the "*glucan trimming*" hypothesis (Ball et al., 1996) behind the water-insoluble properties of amylopectin could further explain the observed correlations. Briefly, a tightly branched "*pre-amylopectin*" produced by the action of starch synthase (SS) and starch branching enzyme (SBE) isoforms, is trimmed down by the debranching enzyme (DBE). The trimming process occurs simultaneously with two important structural changes: (a) the remaining branches of the

"*preamylopectin*" form the characteristic double helices in the building blocks, and (b) the amylopectin backbone being cleared of several chains is being further elongated (Tetlow & Bertoft, 2020). The inter-block chain length (IB-CL), or the segment between successive building blocks, could affect the crystallinity of the resulting amylopectin supramolecular structure, whereby shorter IB-CL limits parallel packing of double helices leading to low onset gelatinization temperature characteristic of decreased crystallinity (Vamadevan, Bertoft, & Seetharaman, 2013). The possibility that backbones of interlinked AM2 (DP > 120) accommodate longer IB-CL (more crystalline amylopectin structures) than MCAP (DP 37–120) backbones could potentially explain their opposing correlations with GI. Similarly, RS negatively correlated with MCAP only ($p < .05$), while the latter negatively correlated with AM1 and AM2, and positively with SCAP1 and SCAP3 ($p < .05$). Still based on the backbone model (Vamadevan et al., 2013), short IB-CL is thought to be associated with higher number of building blocks per cluster which may explain positive correlation between MCAP and SCAP, whereas longer IB-CL (which we hypothesize to be correlated with AM2) had fewer building blocks and may thus explain the strong negative correlation between AM1 and fractions MCAP and SCAP. The propensity of a rice cultivar to form more AM2 than MCAP backbone as the amylopectin chains are being trimmed and elongated could lead to a more stable crystalline structure with fewer amylopectin short chain double helices and thus lower GI. Consistent with this, moderate RS lines were determined to have elevated AM2 as compared to other starch regions (Parween et al., 2020).

3.2. Evaluation of in vitro digestion methods for GI prediction

The soundness of the most widely used Method 1 (Goñi et al., 1997) as an *in vitro* method to predict the GI was evaluated using the same set of milled rice samples with known *in vivo* GI. It was compared to a second *in vitro* method (Alhambra et al., 2019) previously used for in-house GI screening. Finally, a slightly modified version of the simulated digestion method by Germaine et al. (2008) employing lower enzyme concentrations than Method 2 was used. The components of each method are summarized in Table 2.

As a starting point, Method 1 was employed to predict GI based on starch hydrolysis rate at 90 min (SH90) and HI, as previously employed in other studies (Deepa et al., 2010; Fernandes et al., 2020; Kale et al., 2015; Kunyanee & Luangsakul, 2018). By the end of the digestion period, hydrolyzed starch values ranged between 63.96% (IRRI163) to 75.40% (IR65). As shown in the corresponding digestion curves in Fig. 2a, only IR64 and IR65 are clearly separated from the rest, whereas both intermediate and low GI lines are grouped together in a narrow range of SH values despite the huge differences in their *in vivo* GI values. Strong correlations with *in vivo* GI (Pearson correlation coefficient, *r*; Fig. 3a) were found between various SH (SH60-SH120 with r = 0.76-0.86) and all AUC (r = 0.82-0.86, except for AUC(120–180)) ($p < .05$, Table S2), while a very strong correlation was found for SH30 (r = 0.90, $p = .005$). The limitation of Method 1 to separate the groups was made apparent when equations 1 and 2 are applied using single-point hydrolysis rate SH90 and hydrolysis index HI (encompassing 0–180 min), respectively (Fig. 3c and Fig. A1). Actual *in vivo* GI values ranged between 50.4 and 90, while predicted GI values using equations 1 and 2 (pGI_{1a} and pGI_{1b}, respectively) fall between 64.9-71.1 and 66.9–73.0, respectively. Consequently, the plot between pGI_{1a} and pGI_{1b} and *in vivo* GI only achieved R^2 values of 0.732 and 0.690.

To check whether the more intact grains will improve the separation of digestion profiles, Method 1 was slightly modified (referred as Modified Method 1). As hypothesized, a significant improvement in the separation of digestion curves according to GI categories (Fig. 2b) and correlation with GI (Fig. 3b) was established for all SH and AUC parameters in the modified method compared to that of the Method 1 (Figs. 2a and 3a). Among the AUC ranges, highest correlation was established between GI and AUC (30–60) ($r = 0.97$, $p < .001$) for which the linear relationship is described by the equation $pGI_{1c} = 0.04 \times AUC(30–60) + 43.86$ ($R^2 = 0.932$, Fig. 3d).

Simultaneously, Method 2 was performed to test whether well-resolved digestion profiles consistent with the trend in the GI of the samples would be achieved. Final hydrolysis rates were between 49.73% (IRRI147) and 60.08% (IR65), as presented in Fig. 2c. It showed better separation during the first 60 min according to *in vivo* GI values, resulting to higher positive correlation with GI (with r = 0.93-0.95 between 0 and 10 min and r = 0.77-0.89 between 10 and 60 min, $p < .01$-.05, Fig. 4a), while succeeding time points had no significant correlation with GI. AUC(0–5) achieved the highest correlation with GI ($r = 0.96$, $p = .0007$) and this linear relationship is represented by the equation $pGI_2 = 0.44 \times AUC(0–5) + 33.43$ ($R^2 = 0.917$, Fig. 4c).

Fig. 2d shows the digestion curves of the same samples when subjected to Method 3 which produced better separation between GI groups compared to Method 1 and 2. In contrast to the previous methods, Method 3 produced a gradual increase in starch digestion rates between 0 and 180 min, with final values ranging between 16.78% (IRRI147) and 57.66% (IR65). Curves for GQ02522, GQ02497, and IRRI147 (GI = 50.4–55.1), and IRRI163 and IR64 (GI = 64–66) were clustered accordingly while that of IR65 (GI = 90) was clearly separated from the rest. Correlation of the SH values and corresponding AUCs calculated from successive time point ranges with *in vivo* GI (Fig. 4b, Table S5) was highest for SH180 ($r = 0.980$, $p < .001$) and AUC (150–180 min) ($r = 0.976$, $p < .001$). A good linear relationship between *in vivo* GI and AUC (150–180) is described by the equation $pGI_3 = 0.031 \times AUC(150–180) + 37.60$ ($R^2 = 0.953$) to estimate GI based on AUC(150–180) as shown in Fig. 4d. However, it is important to note that very high significant correlations were also established using any of the SH and AUC values, with the lowest being $r = 0.957$ for AUC(0–30). Moreover, it should be noted that SH180 values of Method 3 (16.78%–30.60%, excluding IR65) fall within the SH10 values of Method 2, which may be due to the higher enzyme concentration and conceivably higher digestion rates in the latter (Table 2). This also explains higher SH/AUC correlations with GI established at earlier time points in Method 2. As observed with the various starch structure parameters (Section 3.1), selected simulated digestion variables AUC(0–5) from Method 2 and AUC(150–180) from Method 3 comply with the assumptions of linear regression (Table 3).

Various *in vitro* enzymatic digestion conditions such as enzyme concentration and sample form affect the rate of starch digestion (Woolnough, Monro, Brennan, & Bird, 2008) and may explain the observed discrepancy across the three methods. In contrast to the first

Table 2
Summary of the steps and components of the simulated digestion methods used for *in vitro* GI prediction.

Step	Method 1	Method 2	Method 3
Cooking	50 ± 0.1 mg flour +3 mL water	500 ± 10 mg milled grains +6 mL water (excess water discarded after cooking)	300 ± 3 mg milled grains +0.6 mL water
Amylase	–	37.5 U/0.5 mL digestion medium (75 U/mL[a])	111 U/3 mL digestion medium (37 U/mL[a])
Incubation	–	20 s, 37 °C	75 s, 37 °C, 60 rpm
Pepsin	0.93 mg (40 U; 3.03 U/mL[a])	5 mg (17,820 U; 3240 U/mL[a]	1.47 mg (63 U; 7 U/mL[a])
Incubation	60 min, 40 °C, 90 rpm	30 min, 37 °C, 200 rpm	30 min, 37 °C, 120 rpm
Amylase or **Pancreatin-AMG**	2.6 U amylase/ 30 mL digestion medium (0.087 U/mL[a])	10 mg Pancreatin-127 U AMG/35.5 mL digestion medium (0.28 mg/mL[a], 3.57 U/mL[a])	0.35 mg Pancreatin-195 U AMG/39 mL digestion medium (0.009 mg/mL[a], 5 U/mL[a])
Incubation	180 min, 37 °C, 120 rpm	180 min, 37 °C, 700 rpm	180 min, 37 °C, 120 rpm

[a] Final concentration in the digestion medium.

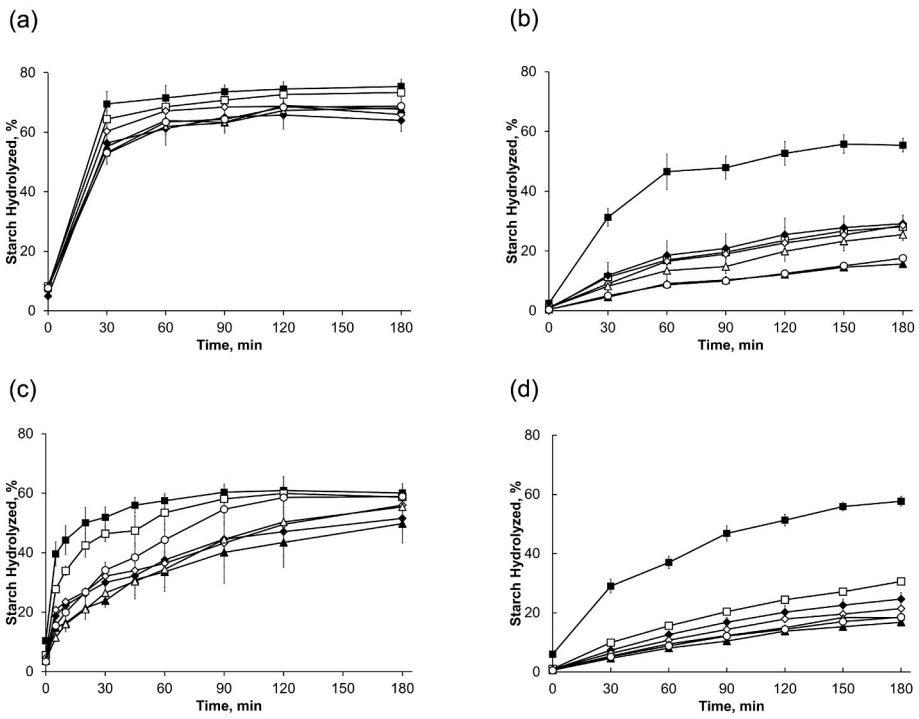

Fig. 2. Percentage of starch hydrolyzed in various samples during simulated digestion using (a) Method 1, (b) modified Method 1, (c) Method 2, and (d) Method 3. The samples and their corresponding *in vivo* GI values are represented as follows (in decreasing order): (—■—) IR65, GI = 90; (—□—) IR64, GI = 66; (—◆—) IRRI163, GI = 64; (—◇—) IRRI162, GI = 57; (—▲—) IRRI147, GI = 55; (—△—) GQ02497, GI = 51.5; (—○—) GQ02522, GI = 50.4. The bars represent standard errors of the mean (SEM) using three (3) to five (5) replicates.

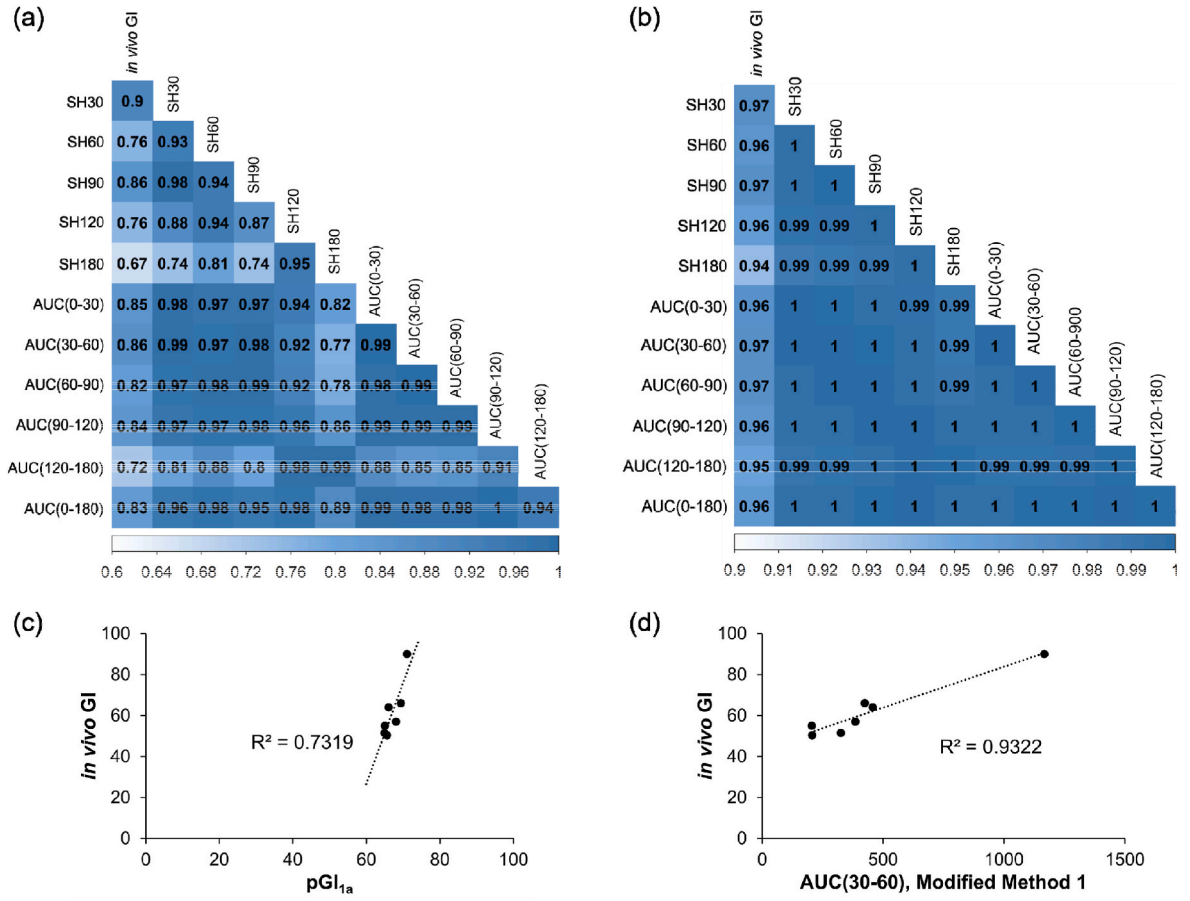

Fig. 3. Correlation matrix showing the association between *in vivo* GI and SH and AUC at various time points and ranges measured in (a) Method 1 and (b) modified Method 1, and the corresponding linear regression plots between *in vivo* GI and (c) predicted GI values (pGI_{1a}) using the single time point equation by Goñi et al. [9] ($pGI_{1a} = 39.21 + (0.803 \times SH90)$; converted from white bread to glucose as reference by multiplying by 0.71, or setting GI = 71 for white bread), and (d) AUC(30–60) from the modified Method 1 to derive the new equation $pGI_{1c} = 0.04 \times AUC(30–60) + 43.86$.

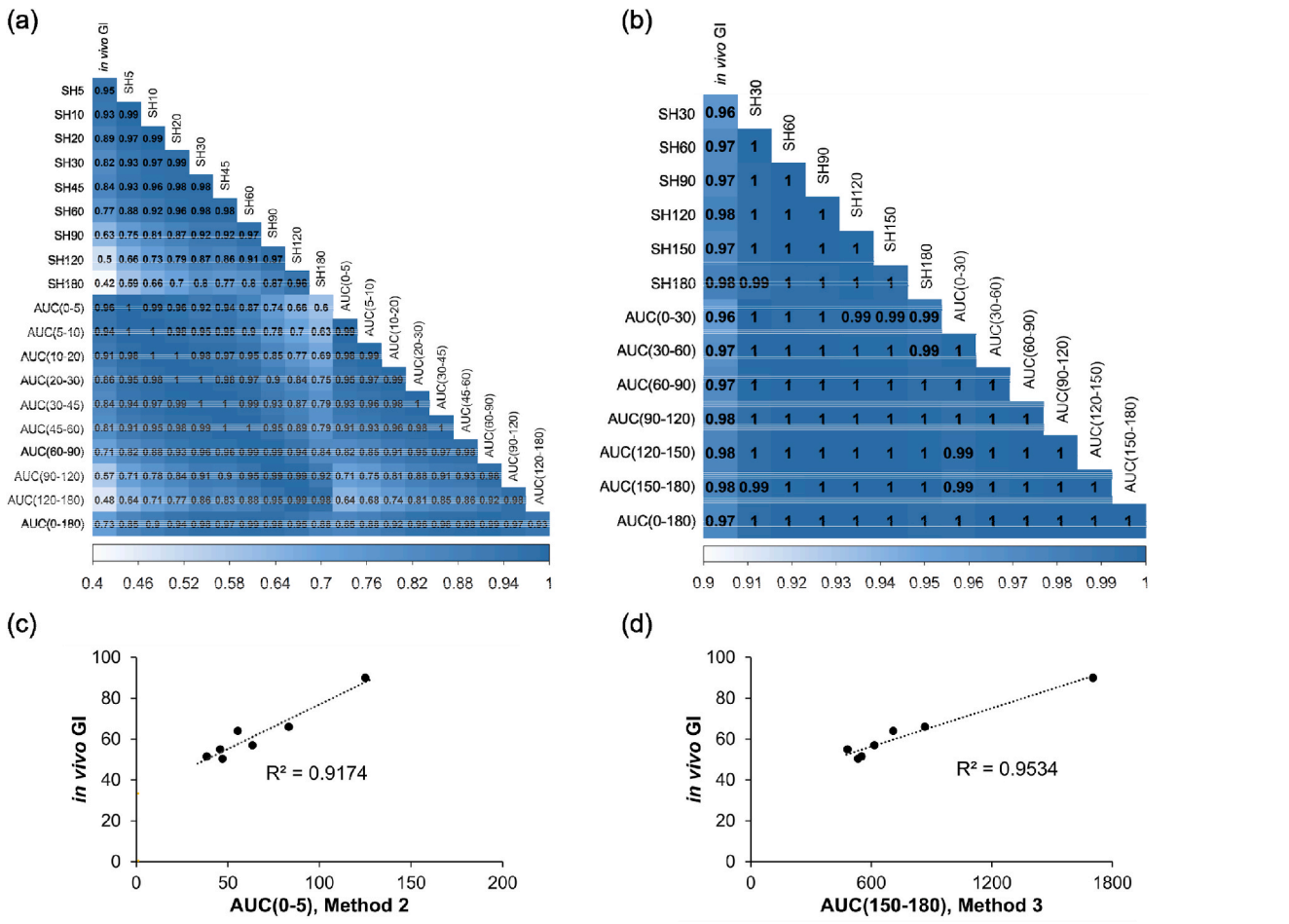

Fig. 4. Correlation matrix describing the association between *in vivo* GI and SH and AUC at various time points and ranges measured in (a) Method 2 and (b) Method 3, and their corresponding linear regression plots between *in vivo* GI and (c) AUC(0–5) from the Method 2 and (d) AUC(150–180) from Method 3 to derive the equations for predicted GI (pGI_2 and pGI_3, respectively).

Table 3
Summary of pGI equations derived in the study using selected parameters.

Linear Regression		ANOVA		Shapiro-Wilk		Breusch-Pagan	
	R^2	F-value	*p* value[a]	W-stat	*p* value[b]	BP value	*p* value[c]
$pGI(RS) = -18.42 \times RS + 87.30$	−.809	9.470	.028	.939	.629	0.885	.347
$pGI(AM1) = -3.96 \times AM1 + 92.16$	−.941	38.657	.002	.909	.393	1.773	.183
$pGI(AM2) = -3.47 \times AM2 + 94.65$	−.802	9.017	.030	.914	.428	2.800	.094
$pGI(MCAP) = 5.33 \times MCAP - 82.85$	.780	7.782	.038	.913	.414	2.074	.150
$pGI(SCAP) = 2.48 \times SCAP - 76.12$	.855	13.557	.014	.899	.326	3.496	.062
$pGI(SCAP1) = 10.11 \times SCAP1 - 91.17$	.856	13.688	.014	.894	.296	2.869	.090
$pGI(AM) = -1.92 \times AM + 94.71$	−.886	18.326	.008	.955	.775	3.185	.074
$pGI(AM_{AUC}) = -1.89 \times AM_{AUC} + 90.67$	−.880	17.114	.009	.939	.631	3.390	.066
$pGI_2 = 0.44 \times AUC(0–5) + 33.43$	.917	38.282	.002	.904	.357	1.960	.162
$pGI_3 = 0.031 \times AUC(150–180) + 37.60$	.953	102.361	<.001	.963	.845	1.038	.308
$pGI(M) = (0.021 \times AUC^{d}) - (1.66 \times AM1) + 58.65$	.995	403.2	<.001	.880	.227	2.483	.289

[a] <.05 corresponds to compliance with linearity assumption.
[b] .05 corresponds to compliance with normal distribution of the residuals of linear regression.
[c] .05 corresponds with compliance to homoscedasticity.
[d] AUC(150–180) from Method 3. The summary of linear regression analysis is presented in Tables A5-A.14.

two methods which produced high starch hydrolysis rates at the onset of the digestion period, Method 3 induced slower digestion as well as lower final SH across samples. This could be attributed to food matrix integrity. For instance, the use of cooked rice flour in Method 1 may have caused the high onset SH across all samples despite the use of lower units of α-amylase (0.087 U/mL digestion medium) compared to that of Method 2 (11.3 U/mL) and Method 3 (0.441 U/mL), and even in the absence of AMG and initial α-amylase digestion. Meanwhile, although both Method 2 and 3 made use of whole milled grain samples, the use of higher amounts of enzymes at all three stages in the former most likely caused the higher SH values, despite the higher AMG concentration in Method 3. In addition, this effect may have been compounded by the fact that Method 2 employed excess water in the cooking step and possible increased mechanical breakdown due to higher stirring speed. The same

effect of cooking in excess water on starch digestibility has been observed in previous studies (Hsu, Lu, Chang, & Chiang, 2014; Huynh, Shrestha, & Arcot, 2016). It is highly likely that higher SH also will have been measured if the excess water used for cooking in Method 2 was not discarded, since amylose and amylopectin leach out of the starch granules upon cooking (Ong & Blanshard, 1995). In this regard, we hypothesize that certain levels of enzyme concentrations, to some extent, is only of secondary importance to matrix integrity when it comes to affecting starch digestibility. Overall, the use of whole milled grain, lower water-to-rice ratio (2:1 vs in excess), and lower enzyme activities in Method 3 may have produced the more gradual and lower extent of starch hydrolysis compared to both Method 1 and 2. In fact, modifying Method 1 by simply employing whole grains (100 mg) and 1:2 water to rice ratio, instead of rice flour and excess water, respectively, led to the establishment of higher correlations with *in vivo* GI (Fig. 2b), thereby supporting this hypothesis.

The discrepancy between the correlations with GI established by starch fine structure components and simulated digestion of more intact starting material may highlight the importance of the overall macro- and micro-structures in the release of glucose from starch over the total content of amylose and amylopectin alone (Chi et al., 2021). For instance, the distribution of DP within amylose and amylopectin chains have been found to influence digestibility; higher short-medium amylose were found to be associated with lower digestibility (Gong, Cheng, Gilbert, & Li, 2019; Yu, Tao, & Gilbert, 2018) due to their tendency upon retrogradation to form smaller and densely packed gel networks that are less accessible to amylolytic enzymes (Yu et al., 2018). With respect to amylopectin, short-chain double helices (DP 6–12) are generally positively associated with increased digestibility while DP 25–36 and DP $\geq$ 37 are known to reduce it (Lin et al., 2016; Srichuwong et al., 2005). However, these fractions could behave otherwise; short helices (DP 6–12) may contribute to the slowly digestible starch (SDS) fraction by either packing into ordered structures (Lin et al., 2016) or promoting steric hindrance against proper enzyme-substrate complex formation (Li & Zhu, 2017), while long-chain helices may comprise the readily digestible starch (RDS) fraction when not in an ordered structure (Kim et al., 2020; Zhang, Ao, & Hamaker, 2008). Going up the hierarchical starch structure, short-range ordered structures associated with SDS and RS (Chi et al., 2019), and starch-complexes with non-starch moieties such as hydrocolloids, proteins, and phenolics decrease digestibility due to localized molecular interactions upon cooking (Chen et al., 2019). Densely-packed single and double helices by amylose and amylopectin, respectively, form different crystalline structures A-, B-, C-, and V-type (starch-hydrophobic molecule complexes) categorized to have high, low, intermediate digestibility and resistant, respectively. Due to the less dense structures of B- and C-type starch crystals that allow for the incorporation of water molecules, they are less readily digested compared to A-type (Shrestha et al., 2012). It was reported that cereals of low to normal amylose content had proportionally high content of A-type crystals with high short:long amylopectin ratio (DP < 24: DP > 36), B-type crystals with longer amylopectin side chains were found in potato starch, while high-amylose starches in cereal and pea had intermediate proportions (Martens et al., 2018). It was also reported in the same study that both %A-type structure and amylopectin side-chain length distribution were the only parameters among those tested (amylose content, granule size, and number of pores) that explicitly predicted the variations in starch digestion kinetics (*in vitro* pig model) across selected botanical types (rice, barley, corn, wheat, potato and pea). Thicker crystalline lamellae relative to the amorphous lamella (where disordered amylose and amylopectin chains are located), highly-ordered reassembled aggregates, and granule surface proteins and lipids are all associated with reduced digestibility. In essence, orientations at various levels of the starch hierarchical structure that limits or slows down enzyme action reduce starch digestibility (Chi et al., 2021).

High rates of digestion due to high enzyme concentration and reduced food matrix macro-structure in both Method 1 and 2 may have diminished the inherent variations in starch fine structure and other inherent hierarchical structures across samples, with SH almost reaching a plateau at earlier time points. In contrast, the more intact samples digested at lower pancreatin and AMG concentrations (as in Method 3) may have introduced lower digestion rates that best reflected SCAP DP variations. For instance, it can be observed that final SH in Method 3 were substantially below %TS content and may likely include mostly SCAP digestion. This can be supported by the results from Benmoussa et al. (2007), where they determined that amylopectin fine structure distribution affects *in vitro* digestibility of rice cultivars, although their results showed a negative correlation between MCAP and RDS.

To establish an *in vitro* GI method that can predict *in vivo* values with higher accuracy, SH and AUC measured from *in vitro* digestion of milled grains are thus superior parameters to use than starch fractions (Fig. 5). This could be due to the ability of the method to account for the effects of various starch parameters (AM1, AM2, SCAP2, RS) and other underlying factors such as the presence of starch-lipid and starch-lipid-protein complexes (Wang et al., 2020), dietary fiber (Qi, Al-Ghazzewi, & Tester, 2018), phenolic compounds (Giuberti, Rocchetti, & Lucini, 2020; Zhu, 2015) which are known to affect starch digestibility and thus GI. Although the use of the single time-point measurement (SH) poses an advantage over AUC measurements with respect to throughput, the use of the latter is less sensitive to errors than SH and is therefore more preferred. The earlier time points of Method 3 (e.g. 0–30 min) can also be used without significantly affecting the predicted GI (R^2 = 0.91, Fig. A3). The comparison of three different *in vitro* digestion methods and fitting the results into models suggests that both Method 2 and Method 3 show potential as *in vitro* screening methods for GI in rice. However, their full utility as an alternative to *in vivo* measurements is remains to be further explored involving large number of varieties with *in vivo* GI evidence.

3.3. Evaluation of the predictive capacity of linear regression models for GI

A summary of the equations derived from the various methods and parameters which showed statistically significant correlation with *in vitro* GI were then used to calculate the pGI of the seven samples of known *in vivo* GI (Table 4), where pGI(AM1), pGI_2 and pGI_3 equations gave GI values with less than 7% mean percentage error (MPE = 6.6%, 5.4%, and 4.0%, respectively). Interestingly, a multiple linear regression model built from AUC(150–180) of Method 3 and AM1 (Table A.15) and described by the equation pGI(M) = (0.021 × AUC(150–180)) – (1.66 × AM1) + 58.65 (R^2 = 0.995, $p < .001$) gave an MPE of only 1.1%. This implies increased predictive capacity when multiple parameters that strongly correlate with GI are used. This result was not surprising given that SEC provides details on the fine structure while simulated digestion could account for the macro- and micro-structure of the food matrix.

Bland-Altman plots (Fig. 5) show the bias (deviation from an ideal mean difference of zero) and agreement limits (within which 95% of differences between the two methods lie) (Giavarina, 2015) between *in vivo* GI and pGI when selected parameters obtained for the 7 samples were fitted in their corresponding linear regression model (except for pGI_{1a} which was calculated using the equation by Goñi et al., 1997). Another set of *in vitro* values (pGI_4, measured at the Commonwealth Scientific and Industrial Research Organization (CSIRO) and extracted from Anacleto et al. (2019) was also evaluated (Fig. A4h). In terms of the mean of differences, most of the models gave a zero bias (or mean difference of 0) except for pGI_{1a} and pGI_{1b} (−5.2 and −7.0 units) and pGI_4 (+3.8 units), indicating that the said *in vitro* methods will give estimates that are 5.2 and 7.0 units higher, and 3.8 units lower, respectively, than *in vivo* values. In terms of the range of differences between *in vitro* and *in vivo* values, the linear regression model with the most accurate agreement range with *in vivo* GI was observed for pGI_3 (−6.0 to 6.0 GI units), which means that 95% of *in vitro* GI measurements will differ by ±6.0

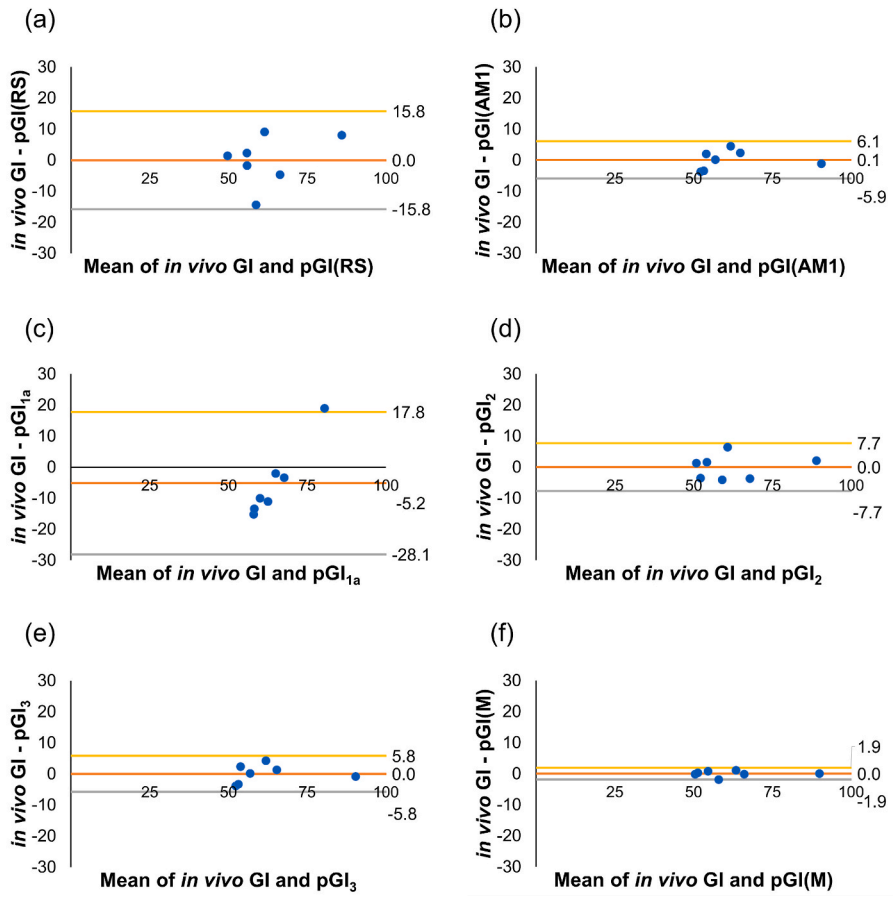

Fig. 5. Bland-Altman plots for (a) pGI(RS), (b) pGI (AM1), (c) pGI_{1a}, (d) pGI_2, (e) pGI_3, and (f) pGI(M) showing the differences between their estimated values and *in vivo* GI vs. the mean of both measurements. The middle horizontal line represents the "bias" (deviation from an ideal mean difference of zero) while top and bottom horizontal lines represent upper and lower limits within which 95% of the differences will fall (calculated as bias ± 1.96 std. deviation, respectively). pGI(M) is a multiple linear regression model derived AUC(150–180) of Method 3 and AM1.

Table 4
pGI values of the seven (7) standard rice samples using various regression models.

Predicted GI	Rice Samples							
	GQ0255	GQ02497	IRRI147	IRRI162	IRRI163	IR64	IR65	MPE[a]
pGI(RS)	49.1 ± 5.1	65.9 ± 15.0	56.7 ± 2.6	54.6 ± 8.4	68.6 ± 4.6	56.9 ± 7.0	81.9 ± 0.9	9.7
pGI(AM1)	46.8 ± 8.3	47.4 ± 5.6	58.0 ± 5.8	62.7 ± 9.3	67.7 ± 5.4	67.7 ± 9.2	83.6 ± 5.1	6.6
pGI(AM2)	45.3 ± 6.7	51.8 ± 8.1	56.4 ± 0.1	66.0 ± 2.5	71.6 ± 7.1	67.8 ± 4.0	74.9 ± 4.3	8.7
pGI(MCAP)	49.5 ± 4.0	54.4 ± 2.9	57.8 ± 2.1	68.5 ± 9.9	70.2 ± 6.4	54.6 ± 3.8	79.0 ± 3.6	10.3
pGI(SCAP)	46.4 ± 1.7	49.1 ± 10.7	57.5 ± 2.7	62.3 ± 4.5	68.7 ± 3.9	73.2 ± 3.3	76.8 ± 4.6	8.5
pGI(SCAP1)	44.4 ± 4.0	49.9 ± 6.5	61.3 ± 0.1	64.1 ± 1.3	70.5 ± 12.8	65.1 ± 2.8	78.7 ± 3.5	9.0
pGI(AM)	45.4 ± 1.1	49.3 ± 7.2	57.0 ± 2.9	64.6 ± 3.8	70.1 ± 5.3	68.0 ± 3.1	79.6 ± 3.5	7.9
$pGI(AM_{AUC})$	44.8 ± 1.7	51.1 ± 5.9	56.5 ± 3.5	64.2 ± 4.3	71.7 ± 1.0	66.3 ± 3.0	79.5 ± 3.5	7.3
pGI_2	53.9 ± 2.7	50.2 ± 0.3	53.4 ± 2.5	61.1 ± 0.3	57.6 ± 0.6	69.7 ± 3.1	87.9 ± 13.3	5.4
pGI_3	54.3 ± 2.7	54.8 ± 1.1	52.6 ± 1.8	56.8 ± 1.4	59.8 ± 4.4	64.7 ± 2.2	90.9 ± 2.6	4.0
pGI(M)	50.6 ± 1.8	51.2 ± 0.7	54.2 ± 1.2	58.9 ± 0.9	62.9 ± 2.9	66.2 ± 1.5	90.0 ± 1.7	1.1
in vivo GI	50.4	51.5	55	57	64	66	90	–

[a] Mean percentage error.

units compared to the mean of the two measurements. In contrast, wider agreement intervals measured from the bias were observed for the following (in increasing order): pGI(AM1) (±6.0), pGI(AM2) (±6.2), pGI (AM) (±6.3), $pGI(AM_{AUC})$ (±6.4), pGI(SCAP1) (±6.5), pGI(SCAP) (±6.8), pGI(MCAP) (±7.2), pGI_2 (±7.7), pGI_4 (±11.7), pGI(RS) (±15.8), pGI_{1a} (±22.9), and pGI_{1b} (±23.2). Notably higher predictive capacity was observed for the multiple regression equation pGI(M), achieving a narrow ±1.9 units of agreement interval.

Receiver operating characteristic (ROC) curves (Fig. 6) were generated for pGI(AM1), pGI_2, and pGI_3 using individual replicates for the seven rice accessions to graphically illustrate their ability to predict *in vivo* values. For this purpose, pGI measurements that fell within ±1 to ±10 units (at increments of ±1) from the *in vivo* GI were classified as "passed", and otherwise, "failed". Based on AUROC (Hosmer et al., 2013), both pGI(AM1) and pGI_2 gave acceptable predictions while pGI_3 has an excellent predictive ability. Interestingly, the multiple linear regression model pGI(M) derived from the parameters AM1 and AUC (150–180) of Method 3 gave and outstanding prediction of GI. These results further support the conclusion that these models may be further explored for the potential to predict GI at acceptable capacities or levels.

A total of 10 market samples were then used to demonstrate the phenotypic variability of estimated GI across different methods (Table 3). Models pGI(AM1), pGI(MCAP), and pGI_3 were able to predict GI values that are close to that reported for low-GI rice (LGR) at 49.9, 45.8, and 55.3, respectively (Table 5). Estimates of GI for Iddly rice (IR) were also within, or at least close to, the low GI range except for pGI(RS)

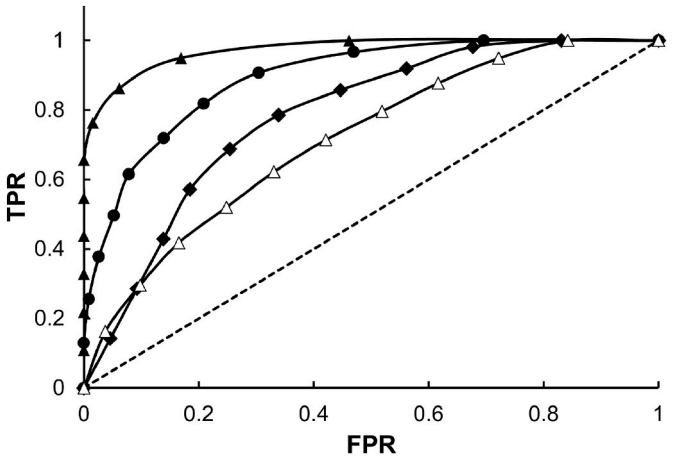

Fig. 6. Receiver operating characteristic (ROC) curves comparing the *in vitro* GI values obtained using linear regression models pGI(AM), pGI_2, pGI_3, and pGI (M) against *in vivo* GI. A single measurement using either method was categorized as "passed" (otherwise, "failed") when it is within ±1 up to ±10 GI units (at increments of ±1 unit) of the *in vivo* value of the seven (7) rice samples used. pGI(M) is a multiple linear regression model derived AUC(150–180) of Method 3 and AM1. The area under the respective ROCs are as follows (in increasing order): (—) chance diagonal, 0.5; (—△—) pGI(AM1), 0.714; (—◆—) pGI2, 0.781; (—●—) pGI3, 0.891; and (—▲—) pGI(M), 0.969. Interpretation: 0.5 < ROC <0.7 = poor prediction; 0.7 ≤ ROC <0.8 = acceptable prediction; 0.8 ≤ ROC <0.9 = excellent prediction; ROC ≥0.9 = outstanding prediction (Hosmer, Lemeshow, & Sturdivant, 2013); TPR = True Positive Rate; FPR = False Positive Rate.

and pGI_2 which gave higher values. All models were able to assign high GI values for both glutinous white and black rices (GWR and GBR) which is expected for waxy rices (Kaur et al., 2016). All models also classified the Jasmine rices (WR and BJR) accordingly as high GI cultivars, while Thai Red as intermediate to high. Meanwhile, the Basmati rices (LBR and BR) got low to high pGI values. The differences in pGI using eight models was smallest for Extra-Long Basmati Rice (LBR), differing at least 10.1 units, while the pGI for White Glutinous Rice (WGR) and Black Glutinous Rice (BGR) varied for more than 40 units across models, highlighting the variability of the predictive capacities of different methods, and thus, the need to come up with the most accurate one.

4. Conclusion

This work aimed to establish an *in vitro* method for GI screening in rice by exploring the use of amylolysis, starch indices, and starch fractions as parameters for GI prediction. This study demonstrated that resistant starch (RS), amylose (AM1, DP > 1000, and AM2, 121 < DP ≤ 1000), and short-chain amylopectin (SCAP, particularly SCAP of DP 25–36) are strongly to very strongly correlated with *in vivo* GI. Meanwhile, higher correlations were observed for SH and AUC measured through modified *in vitro* amylolysis protocol employing intact grains, low sample requirements, and lower enzyme activities, even within shorter digestion periods of 5 and 30 min. However, lower mean percentage errors were achieved when AUC(150–180) and AM1 were combined into a multiple regression model. We conclude that simulated digestion Method 3 can be explored for in predicting the GI in closer to *in vivo* situation. We infer that amylolysis of cooked whole milled grains at conditions that do not diminish the effect of grain structural integrity (whole milled grain, lower rice-to-water ratio during cooking, and lower concentration of amylolytic enzymes) and thus improved *in vitro* methods exhibit more accurate predictive capacity than the use of more specific starch indices and starch fractions. This could be due to the ability of digestion models, with certain incubation conditions, to simultaneously account for differences in various factors (e.g. SCAP2 and AM2, starch-lipid and starch-lipid-protein complexes, and enzyme-inhibiting phytochemicals) affecting starch digestibility. However, AM1 data can further improve predictive capacity. In addition, we found that previously reported pGI equations did not accurately predict *in vivo* GI for the rice accessions used in this study, and hence, the need to generate more accurate pGI equations specific to an *in vitro* digestion protocol, which was demonstrated herein. Future studies involving higher number of samples with profiles on protein, lipids, and phenolics content, and more variety of botanical sources could be used to overcome some of the limitations of the current study.

Table 5
Predicted GI (pGI) values of market samples across various pGI models.

Samples	GI	Predicted GI				
		pGI(RS)	pGI (AM1)	pGI (AM2)	pGI (MCAP)	pGI (SCAP)
IR	38[a]	61.7 ± 5.1	37.7 ± 0.6	59.8 ± 0.4	41.7 ± 1.9	54.6 ± 1.6
CR	83[a]	77.4 ± 2.5	57.2 ± 3.9	75.7 ± 2.0	55.1 ± 2.3	72.0 ± 4.9
LGR	54[a]	73.4 ± 2.0	49.9 ± 2.0	70.1 ± 0.0	45.8 ± 2.3	67.7 ± 2.3
LBR	52[a]	68.6 ± 7.9	56.3 ± 4.8	71.2 ± 2.4	58.7 ± 6.0	66.6 ± 7.5
BR	50[b]/ 58[c]	76.3 ± 0.7	63.7 ± 2.7	70.9 ± 1.1	55.9 ± 4.7	72.3 ± 1.3
WR	91[a]	79.1 ± 3.7	79.3 ± 0.2	80.6 ± 2.9	79.0 ± 18.2	78.2 ± 10.4
WGR	93[a]	80.9 ± 2.8	91.2 ± 0.2	92.3 ± 2.0	115.2 ± 9.0	77.3 ± 5.7
BGR	42[a]/ 74[d]	80.5 ± 2.4	86.8 ± 2.1	90.8 ± 0.2	103.7 ± 12.3	78.7 ± 7.1
TRR	76[d]	78.9 ± 0.8	68.5 ± 19.8	71.3 ± 15.4	81.0 ± 7.4	63.9 ± 20.0
BJR	74	81.0 ± 1.5	86.1 ± 0.4	87.6 ± 2.9	80.7 ± 3.8	86.6 ± 3.6
Samples		**pGI (SCAP1)**	**pGI (AM)**	**pGI (AM_{AUC})**	**pGI_2**	**pGI_3**
IR	38[a]	49.9 ± 1.2	49.0 ± 0.5	47.9 ± 0.7	63.0 ± 15.0	57.7 ± 0.7
CR	83[a]	68.2 ± 2.5	67.2 ± 3.0	65.5 ± 3.2	90.0 ± 6.6	74.8 ± 2.1
LGR	54[a]	58.7 ± 0.5	60.6 ± 1.0	59.2 ± 0.8	56.6 ± 0.6	55.3 ± 0.4
LBR	52[a]	65.5 ± 2.8	64.4 ± 3.6	63.5 ± 3.4	51.6 ± 11.0	64.9 ± 0.1
BR	50[b]/ 58[c]	68.5 ± 2.4	67.8 ± 0.7	66.8 ± 0.6	58.4 ± 0.4	72.6 ± 1.2
WR	91[a]	83.8 ± 1.4	80.7 ± 1.5	79.1 ± 1.4	67.5 ± 4.2	74.4 ± 1.0
WGR	93[a]	106.9 ± 3.6	93.0 ± 1.2	89.8 ± 0.5	93.2 ± 3.2	97.8 ± 0.0
BGR	42[a]/ 74[d]	105.0 ± 2.6	90.0 ± 1.1	86.8 ± 1.3	48.4 ± 9.4	68.7 ± 0.3
TRR	76[d]	79.9 ± 20.3	70.3 ± 18.2	64.8 ± 13.8	66.7 ± 5.3	79.3 ± 0.4
BJR	74	100.3 ± 3.6	87.9 ± 1.4	84.4 ± 1.1	71.4 ± 1.6	85.5 ± 0.1

The values are expressed as the mean of three (3) replicates for RS, two (2) for SEC-derived parameters, pGI_2, and pGI_3 ± standard deviation. [a]Based on literature search by Kaur, Lim, Chusak, and Henry (2020); [c]Ranawana, Henry, Lightowler, and Wang (2009); [d]Foster-Powell, Holt, and Brand-Miller (2002); [e]Indrasari, Purwani, Wibowo, and Jumali (2010); IR=Iddly Rice; CR= Premium Calrose Rice; LGR = Kangaroo Australian Low GI Rice; LBR = Extra Long Basmati Rice; BR=Basmati Rice; WR=Thai Hom Mali Premium Quality Fragrant Rice (Jasmine white rice); WGR=White Glutinous Rice; BGR=Black Glutinous Rice; TRR = Premium Thai Red Rice; BJR=Brown Jasmine Rice.

Funding

Nese Sreenivasulu acknowledge the funding support of CGIAR Rice Program, Foundation for food and agriculture research (FFAR),

Department of Agriculture, Philippines (OneRicePH), Temperate Rice Research Consortium and Indian Council of Agriculture Research (ICAR-IRRI work plan). A portion of this work is a component of a PhD dissertation partially funded by the Commission on Higher Education (CHED), Philippines.

Declaration of competing interest

The authors declare that they have no known competing financial interests or personal relationships that could have appeared to influence the work reported in this paper.

CRediT authorship contribution statement

Putlih Adzra Pautong: Methodology, Validation, Formal analysis, Investigation, Writing – original draft. **Joanne Jerenice Añonuevo:** Methodology, Validation, Formal analysis, Investigation, Writing – original draft. **Maria Krishna de Guzman:** Methodology, Validation. **Rodolfo Sumayao:** Conceptualization, Writing – review & editing. **Christiani Jeyakumar Henry:** Writing – review & editing. **Nese Sreenivasulu:** Conceptualization, Writing – review & editing, Visualization, Supervision, Project administration, Funding acquisition.

Data availability

Data will be made available on request.

Acknowledgements

We acknowledge the following individuals for their contributions: Anna Natoza from the Consumer-Driven Grain Quality and Nutrition (CDGQN) Cluster at IRRI who assisted in SEC experiments and other starch-related assays; Luster May Serrano-Labarga from CDGQN for HPLC troubleshooting tips and insightful discussions with PATP; and, Asst. Professor Anna Jean Garcia from the University of Southern Mindanao for her comments on statistical analysis.

Appendix A. Supplementary data

Supplementary data to this article can be found online at https://doi.org/10.1016/j.lwt.2022.113929.

References

Alhambra, C. M., Dhital, S., Sreenivasulu, N., & Butardo, V. M. (2019). Quantifying grain digestibility of starch fractions in milled rice. In N. Sreenivasulu (Ed.), *Methods in molecular biology* (Vol. 1892, pp. 241–252). New York, NY: Humana Press. https://doi.org/10.1007/978-1-4939-8914-0_13.

Anacleto, R., Badoni, S., Parween, S., Butardo, V. M., Misra, G., Cuevas, R. P., et al. (2019). Integrating a genome-wide association study with a large-scale transcriptome analysis to predict genetic regions influencing the glycaemic index and texture in rice. *Plant Biotechnology Journal, 17*(7), 1261–1275. https://doi.org/10.1111/pbi.13051

Atkinson, F. S., Foster-Powell, K., & Brand-Miller, J. C. (2008). International tables of glycemic index and glycemic load values. *Diabetes Care*. https://doi.org/10.2337/dc08-1239, 2008.

Ball, S., Guan, H. P., James, M., Myers, A., Keeling, P., Mouille, G., et al. (1996). From glycogen to amylopectin: A model for the biogenesis of the plant starch granule. *Cell, 86*(3), 349–352. https://doi.org/10.1016/s0092-8674(00)80107-5

Banerjee, S., Chandel, G., Mandal, N., Meena, B., & Saluja, A. (2011). Assessment of nutritive value in milled rice grain of some Indian rice landraces and their molecular characterization. *Bangladesh Journal of Agricultural Research, 36*. https://doi.org/10.3329/bjar.v36i3.9265

Benmoussa, M., Moldenhauer, K. A. K., & Hamaker, B. R. (2007). Rice amylopectin fine structure variability affects starch digestion properties. *Journal of Agricultural and Food Chemistry, 55*(4), 1475–1479. https://doi.org/10.1021/jf062349x

Bertoft, E. (2004). On the nature of categories of chains in amylopectin and their connection to the super helix model. *Carbohydrate Polymers, 57*(2), 211–224. https://doi.org/10.1016/j.carbpol.2004.04.015

Blaak, E. E., Antoine, J. M., Benton, D., Björck, I., Bozzetto, L., Brouns, F., et al. (2012). Impact of postprandial glycaemia on health and prevention of disease. *Obesity Reviews*. https://doi.org/10.1111/j.1467-789X.2012.01011.x

Brodkorb, A., Egger, L., Alminger, M., Alvito, P., Assunção, R., Ballance, S., et al. (2019). INFOGEST static in vitro simulation of gastrointestinal food digestion. *Nature Protocols, 14*(4), 991–1014. https://doi.org/10.1038/s41596-018-0119-1

Brotman, Y., Llorente-Wiegand, C., Oyong, G., Badoni, S., Misra, G., Anacleto, R., et al. (2021). The genetics underlying metabolic signatures in a brown rice diversity panel and their vital role in human nutrition. *The Plant Journal, 106*(2), 507–525. https://doi.org/10.1111/tpj.15182

Butardo, V. M., Anacleto, R., Parween, S., Samson, I., de Guzman, K., Alhambra, C. M., et al. (2017). Systems genetics identifies a novel regulatory domain of amylose synthesis. *Plant Physiology, 173*(1), 887–906. https://doi.org/10.1104/pp.16.01248

Castro, J. V., Dumas, C., Chiou, H., Fitzgerald, M. A., & Gilbert, R. G. (2005). Mechanistic information from analysis of molecular weight distributions of starch. *Biomacromolecules, 6*(4), 2248–2259. https://doi.org/10.1021/bm0500401

Chen, L., Zhang, H., McClements, D. J., Zhang, Z., Zhang, R., Jin, Z., et al. (2019). Effect of dietary fibers on the structure and digestibility of fried potato starch: A comparison of pullulan and pectin. *Carbohydrate Polymers, 215*, 47–57. https://doi.org/10.1016/j.carbpol.2019.03.046

Chi, C., Li, X., Huang, S., Chen, L., Zhang, Y., Li, L., et al. (2021). Basic principles in starch multi-scale structuration to mitigate digestibility: A review. *Trends in Food Science & Technology, 109*, 154–168. https://doi.org/10.1016/j.tifs.2021.01.024

Chi, C., Li, X., Lu, P., Miao, S., Zhang, Y., & Chen, L. (2019). Dry heating and annealing treatment synergistically modulate starch structure and digestibility. *International Journal of Biological Macromolecules, 137*, 554–561. https://doi.org/10.1016/j.ijbiomac.2019.06.137

Chung, H.-J., Shin, D.-H., & Lim, S.-T. (2008). In vitro starch digestibility and estimated glycemic index of chemically modified corn starches. *Food Research International, 41*(6), 579–585. https://doi.org/10.1016/j.foodres.2008.04.006

Deepa, G., Singh, V., & Naidu, K. A. (2010). A comparative study on starch digestibility, glycemic index and resistant starch of pigmented ("Njavara" and 'Jyothi') and a non-pigmented ('IR 64') rice varieties. *Journal of Food Science & Technology, 47*(6), 644–649. https://doi.org/10.1007/s13197-010-0106-1

Edwards, C. H., Cochetel, N., Setterfield, L., Perez-Moral, N., & Warren, F. J. (2019). A single-enzyme system for starch digestibility screening and its relevance to understanding and predicting the glycaemic index of food products. *Food & Function, 10*(8), 4751–4760. https://doi.org/10.1039/C9FO00603F

Englyst, K. N., Vinoy, S., Englyst, H. N., & Lang, V. (2003). Glycaemic index of cereal products explained by their content of rapidly and slowly available glucose. *British Journal of Nutrition, 89*(3), 329–340. https://doi.org/10.1079/BJN2002786

Fernandes, J.-M., Madalena, D. A., Pinheiro, A. C., & Vicente, A. A. (2020). Rice in vitro digestion: Application of INFOGEST harmonized protocol for glycemic index determination and starch morphological study. *Journal of Food Science & Technology, 57*(4), 1393–1404. https://doi.org/10.1007/s13197-019-04174-x

Fitzgerald, M. A., Rahman, S., Resurreccion, A. P., Concepcion, J., Daygon, V. D., Dipti, S. S., et al. (2011). Identification of a major genetic determinant of glycaemic index in rice. *Rice, 4*(2), 66–74. https://doi.org/10.1007/s12284-011-9073-z

Foster-Powell, K., Holt, S. H. A., & Brand-Miller, J. C. (2002). International table of gylcemic index and glycemic load values. *American Journal of Clinical Nutrition*. https://doi.org/10.1093/ajcn/76.1.5, 2002.

Germaine, K. A., Samman, S., Fryirs, C. G., Griffiths, P. J., Johnson, S. K., & Quail, K. J. (2008). Comparison of in vitro starch digestibility methods for predicting the glycaemic index of grain foods. *Journal of the Science of Food and Agriculture, 88*(4), 652–658. https://doi.org/10.1002/jsfa.3130

Giavarina, D. (2015). Understanding Bland Altman analysis. *Biochemia Medica, 25*(2), 141–151. https://doi.org/10.11613/BM.2015.015

Giuberti, G., Rocchetti, G., & Lucini, L. (2020). Interactions between phenolic compounds, amylolytic enzymes and starch: An updated overview. *Current Opinion in Food Science, 31*, 102–113. https://doi.org/10.1016/j.cofs.2020.04.003

Gong, B., Cheng, L., Gilbert, R. G., & Li, C. (2019). Distribution of short to medium amylose chains are major controllers of in vitro digestion of retrograded rice starch. *Food Hydrocolloids, 96*, 634–643. https://doi.org/10.1016/j.foodhyd.2019.06.003

Goñi, I., Garcia-Alonso, A., & Saura-Calixto, F. (1997). A starch hydrolysis procedure to estimate glycemic index. *Nutrition Research*. https://doi.org/10.1016/S0271-5317(97)00010-9

GRiSP (Global Rice Science Partnership). (2013). Rice Almanac: Source book for one of the most important economic activities on earth. In *IRRI* (4th ed.). International Rice Research Institute. Los Baños, Philippines.

Guzman, M. K. de, Parween, S., Butardo, V. M., Alhambra, C. M., Anacleto, R., Seiler, C., et al. (2017). Investigating glycemic potential of rice by unraveling compositional variations in mature grain and starch mobilization patterns during seed germination. *Scientific Reports, 7*(1), 5854. https://doi.org/10.1038/s41598-017-06026-0

Hanashiro, I., Abe, J., & Hizukuri, S. (1996). A periodic distribution of the chain length of amylopectin as revealed by high-performance anion-exchange chromatography. *Carbohydrate Research, 283*, 151–159. https://doi.org/10.1016/0008-6215(95)00408-4

Hosmer, D. W., Jr., Lemeshow, S., & Sturdivant, R. X. (2013). Assessing the fit of the model. In D. W. Hosmer, Jr., S. Lemeshow, & R. X. Sturdivant (Eds.), *Applied logistic regression* (pp. 153–225). https://doi.org/10.1002/9781118548387.ch5

Hsu, R., Lu, S., Chang, Y.-H., & Chiang, W. (2014). Effects of added water and retrogradation on starch digestibility of cooked rice flours with different amylose content. *Journal of Cereal Science, 61*. https://doi.org/10.1016/j.jcs.2014.03.002

Huynh, T. D., Shrestha, A. K., & Arcot, J. (2016). Physicochemical properties and digestibility of eleven Vietnamese rice starches with varying amylose contents. *Food & Function, 7*(8), 3599–3608. https://doi.org/10.1039/C6FO00661B

Hu, P., Zhao, H., Duan, Z., Linlin, Z., & Wu, D. (2004). Starch digestibility and the estimated glycemic score of different types of rice differing in amylose contents. *Journal of Cereal Science, 40*(3), 231–237. https://doi.org/10.1016/j.jcs.2004.06.001

Indrasari, S. D., Purwani, E. Y., Wibowo, P. S. L., & Jumali. (2010). Glycemic indices of some rice varieties. *Indonesian Journal of Agriculture, 3*(1), 9–16.

Jenkins, D. J. A., Wolever, T. M. S., Taylor, R. H., Barker, H., Fielden, H., Baldwin, J. M., et al. (1981). Glycemic index of foods: A physiological basis for carbohydrate exchange. *American Journal of Clinical Nutrition, 34*(3), 362–366. https://doi.org/10.1093/ajcn/34.3.362

Jukanti, A. K., Pautong, P. A., Liu, Q., & Sreenivasulu, N. (2020). Low glycemic index rice—a desired trait in starchy staples. *Trends in Food Science & Technology, 106*, 132–149. https://doi.org/10.1016/j.tifs.2020.10.006

Juliano, B. (1985). *Polysaccharides, proteins and lipids of rice*.

Kale, S. J., Jha, S. K., Jha, G. K., Sinha, J. P., & Lal, S. B. (2015). Soaking induced changes in chemical composition, glycemic index and starch characteristics of Basmati rice. *Rice Science, 22*(5), 227–236. https://doi.org/10.1016/j.rsci.2015.09.002

Kaur, B., Lim, J., Chusak, C., & Henry, C. J. (2020). Microwave cooking enhances glycaemic potential of rice: An in vitro study. *Malaysian Journal of Nutrition, 26*(1), 117–128. https://doi.org/10.31246/MJN-2019-0106

Kaur, B., Ranawana, V., & Henry, J. (2016). The glycemic index of rice and rice products: A review, and table of GI values. *Critical Reviews in Food Science and Nutrition, 56*(2), 215–236. https://doi.org/10.1080/10408398.2012.717976

Kim, H. R., Choi, S. J., Choi, H.-D., Park, C.-S., & Moon, T. W. (2020). Amylosucrase-modified waxy potato starches recrystallized with amylose: The role of amylopectin chain length in formation of low-digestible fractions. *Food Chemistry, 318*, Article 126490. https://doi.org/10.1016/j.foodchem.2020.126490

Kim, H. J., & White, P. J. (2012). In vitro digestion rate and estimated glycemic index of oat flours from typical and high β-glucan oat lines. *Journal of Agricultural and Food Chemistry, 60*(20), 5237–5242. https://doi.org/10.1021/jf300429u

Koroteeva, D. A., Kiseleva, V. I., Sriroth, K., Piyachomkwan, K., Bertoft, E., Yuryev, P. V., et al. (2007). Structural and thermodynamic properties of rice starches with different genetic background Part 1. Differentiation of amylopectin and amylose defects. *International Journal of Biological Macromolecules, 41*(4), 391–403. https://doi.org/10.1016/j.ijbiomac.2007.05.010

Kunyanee, K., & Luangsakul, N. (2018). The utilization of ultrasound and chilling treatment to reduce GI in Thai glutinous rice (RD6). *International Journal of Agricultural Technology, 14*, 1365–1378. https://scholar.google.com/scholar?hl=en&as_sdt=0%2C5&q=Kunyanee%2C+K.%2C+%26+Luangsakul%2C+N.+%282018%29.+The+utilization+of+ultrasound+and+chilling+treatment+to+reduce+GI+in+Thai+glutinous+rice+%28RD6%29.+&btnG=.

Lal, M. K., Kumar, A., Raigond, P., Dutt, S., Changan, S. S., Chourasia, K. N., et al. (2021). Impact of starch storage condition on glycemic index and resistant starch of cooked potato (Solanum tuberosum) tubers. *Starch - Stärke, 73*(1–2), Article 1900281. https://doi.org/10.1002/star.201900281

Leoro, M. G. V., Clerici, M. T. P. S., Chang, Y. K., & Steel, C. J. (2010). Evaluation of the in vitro glycemic index of a fiber-rich extruded breakfast cereal produced with organic passion fruit fiber and corn flour. In *Food science and technology* (Vol. 30, pp. 964–968). scielo.

Lin, L., Guo, D., Huang, J., Zhang, X., Zhang, L., & Wei, C. (2016). Molecular structure and enzymatic hydrolysis properties of starches from high-amylose maize inbred lines and their hybrids. *Food Hydrocolloids, 58*, 246–254. https://doi.org/10.1016/j.foodhyd.2016.03.001

Li, G., & Zhu, F. (2017). Amylopectin molecular structure in relation to physicochemical properties of quinoa starch. *Carbohydrate Polymers, 164*, 396–402. https://doi.org/10.1016/j.carbpol.2017.02.014

Martens, B. M. J., Gerrits, W. J. J., Bruininx, E. M. A. M., & Schols, H. A. (2018). Amylopectin structure and crystallinity explains variation in digestion kinetics of starches across botanic sources in an in vitro pig model. *Journal of Animal Science and Biotechnology, 9*(1), 91. https://doi.org/10.1186/s40104-018-0303-8

Miller, J. B., Pang, E., & Bramall, L. (1992). Rice: A high or low glycemic index food? *American Journal of Clinical Nutrition*. https://doi.org/10.1093/ajcn/56.6.1034

Nakamura, Y. (2018). Rice starch biotechnology: Rice endosperm as a model of cereal endosperms. *Starch - Stärke, 70*(1–2), Article 1600375. https://doi.org/10.1002/star.201600375

Nanditha, A., Ma, R. C. W., Ramachandran, A., Snehalatha, C., Chan, J. C. N., Chia, K. S., et al. (2016). Diabetes in Asia and the Pacific: Implications for the global epidemic. *Diabetes Care, 39*(3), 472. https://doi.org/10.2337/dc15-1536. LP – 485.

Ong, M. H., & Blanshard, J. M. V. (1995). Texture determinants of cooked, parboiled rice. II: Physicochemical properties and leaching behaviour of rice. *Journal of Cereal Science, 21*(3), 261–269. https://doi.org/10.1006/jcrs.1995.0029

Parween, S., Anonuevo, J. J., Butardo, V. M., Jr., Misra, G., Anacleto, R., Llorente, C., et al. (2020). Balancing the double-edged sword effect of increased resistant starch content and its impact on rice texture: Its genetics and molecular physiological mechanisms. *Plant Biotechnology Journal, 18*(8), 1763–1777. https://doi.org/10.1111/pbi.13339

Pasion, E. A., Badoni, S., Misra, G., Anacleto, R., Parween, S., Kohli, A., et al. (2021). OsTPR boosts the superior grains through increase in upper secondary rachis branches without incurring a grain quality penalty. *Plant Biotechnology Journal, 19*(7), 1396–1411. https://doi.org/10.1111/pbi.13560

Perez, S., & Bertoft, E. (2010). The molecular structures of starch components and their contribution to the architecture of starch granules: A comprehensive review. *Starch - Stärke, 62*, 389–420. https://doi.org/10.1002/star.201000013

Qi, X., Al-Ghazzewi, F. H., & Tester, R. F. (2018). Dietary fiber, gastric emptying, and carbohydrate digestion: A mini-review. *Starch - Stärke, 70*(9–10), Article 1700346. https://doi.org/10.1002/star.201700346

Ranawana, D. V., Henry, C. J. K., Lightowler, H. J., & Wang, D. (2009). Glycaemic index of some commercially available rice and rice products in Great Britain. *International Journal of Food Sciences & Nutrition*. https://doi.org/10.1080/09637480802516191

RStudio Team. (2020). *RStudio*. Boston, MA: Integrated Development for R. RStudio, PBC. URL http://www.rstudio.com/.

Shrestha, A. K., Blazek, J., Flanagan, B. M., Dhital, S., Larroque, O., Morell, M. K., et al. (2012). Molecular, mesoscopic and microscopic structure evolution during amylase digestion of maize starch granules. *Carbohydrate Polymers, 90*(1), 23–33. https://doi.org/10.1016/j.carbpol.2012.04.041

Srichuwong, S., Sunarti, T. C., Mishima, T., Isono, N., & Hisamatsu, M. (2005). Starches from different botanical sources I: Contribution of amylopectin fine structure to thermal properties and enzyme digestibility. *Carbohydrate Polymers, 60*(4), 529–538. https://doi.org/10.1016/j.carbpol.2005.03.004

Tetlow, I. J., & Bertoft, E. (2020). A review of starch biosynthesis in relation to the building block-backbone model. *International Journal of Molecular Sciences, 21*(Issue 19). https://doi.org/10.3390/ijms21197011

Toutounji, M. R., Butardo, V. M., Zou, W., Farahnaky, A., Pallas, L., Oli, P., et al. (2019). A high-throughput in vitro assay for screening rice starch digestibility. *Foods, 8*(Issue 12). https://doi.org/10.3390/foods8120601

Toutounji, M. R., Farahnaky, A., Santhakumar, A. B., Oli, P., Butardo, V. M., & Blanchard, C. L. (2019). Intrinsic and extrinsic factors affecting rice starch digestibility. *Trends in Food Science & Technology, 88*(10170), 10–22. https://doi.org/10.1016/j.tifs.2019.02.012

Tutusaus, J. A. M., Srikaeo, K., & Diéguez, J. G. (2013). Effects of amylose and resistant starch on starch digestibility of rice flours and starches. *International Food Research Journal, 20*, 1329–1335.

Vamadevan, V., Bertoft, E., & Seetharaman, K. (2013). On the importance of organization of glucan chains on thermal properties of starch. *Carbohydrate Polymers, 92*(2), 1653–1659. https://doi.org/10.1016/j.carbpol.2012.11.003

Wang, S., Chao, C., Cai, J., Niu, B., Copeland, L., & Wang, S. (2020). Starch–lipid and starch–lipid–protein complexes: A comprehensive review. *Comprehensive Reviews in Food Science and Food Safety, 19*(3), 1056–1079. https://doi.org/10.1111/1541-4337.12550

Wei, T., & Simko, V. (2021). GitHub - taiyun/corrplot: A visual exploratory tool on correlation matrix (Version 0.92). https://github.com/taiyun/corrplot.

Wickham, H., François, R., Henry, L., & Müller, K. (2022). *Dplyr: A grammar of data manipulation*. R package version 1.0.8 https://CRAN.R-project.org/package=dplyr.

Woolnough, J. W., Monro, J. A., Brennan, C. S., & Bird, A. R. (2008). Simulating human carbohydrate digestion in vitro: A review of methods and the need for standardisation. *International Journal of Food Science and Technology*. https://doi.org/10.1111/j.1365-2621.2008.01862.x

World Health Organization. (2020). *Malnutrition*.

World Health Organization. (2021). *Non-communicable diseases*. World Health Organization. https://www.who.int/news-room/fact-sheets/detail/noncommunicable-diseases.

Yan, L. J. (2014). Pathogenesis of chronic hyperglycemia: From reductive stress to oxidative stress. *Journal of Diabetes Research, 2014*. https://doi.org/10.1155/2014/137919

Yu, W., Tao, K., & Gilbert, R. G. (2018). Improved methodology for analyzing relations between starch digestion kinetics and molecular structure. *Food Chemistry, 264*, 284–292. https://doi.org/10.1016/j.foodchem.2018.05.049

Zeileis, A., & Hothorn, T. (2002). Diagnostic checking in regression relationships. *R News, 2*(3), 7–10. URL https://CRAN.R-project.org/doc/Rnews/.

Zhang, G., Ao, Z., & Hamaker, B. R. (2008). Nutritional property of endosperm starches from maize mutants: A parabolic relationship between slowly digestible starch and amylopectin fine structure. *Journal of Agricultural and Food Chemistry, 56*(12), 4686–4694. https://doi.org/10.1021/jf072822m

Zhu, F. (2015). Interactions between starch and phenolic compound. *Trends in Food Science & Technology, 43*. https://doi.org/10.1016/j.tifs.2015.02.003